Development 139, 4524-4535 (2012) doi:10.1242/dev.078261

Non-autonomous crosstalk between the Jak/Stat and Egfr pathways mediates *Apc1*-driven intestinal stem cell hyperplasia in the *Drosophila* adult midgut

Julia B. Cordero[1,*,‡], Rhoda K. Stefanatos[2,*], Kevin Myant[1], Marcos Vidal[2] and Owen J. Sansom[1,‡]

SUMMARY

Inactivating mutations within adenomatous polyposis coli (*APC*), a negative regulator of Wnt signaling, are responsible for most sporadic and hereditary forms of colorectal cancer (CRC). Here, we use the adult *Drosophila* midgut as a model system to investigate the molecular events that mediate intestinal hyperplasia following loss of *Apc* in the intestine. Our results indicate that the conserved Wnt target Myc and its binding partner Max are required for the initiation and maintenance of intestinal stem cell (ISC) hyperproliferation following *Apc1* loss. Importantly, we find that loss of *Apc1* leads to the production of the interleukin-like ligands Upd2/3 and the EGF-like Spitz in a Myc-dependent manner. Loss of *Apc1* or high Wg in ISCs results in non-cell-autonomous upregulation of *upd3* in enterocytes and subsequent activation of Jak/Stat signaling in ISCs. Crucially, knocking down Jak/Stat or Spitz/Egfr signaling suppresses *Apc1*-dependent ISC hyperproliferation. In summary, our results uncover a novel non-cell-autonomous interplay between Wnt/Myc, Egfr and Jak/Stat signaling in the regulation of intestinal hyperproliferation. Furthermore, we present evidence suggesting potential conservation in mouse models and human CRC. Therefore, the *Drosophila* adult midgut proves to be a powerful genetic system to identify novel mediators of *APC* phenotypes in the intestine.

KEY WORDS: Apc, *Drosophila* midgut, Egfr, Myc, Stat, Intestinal stem cells

INTRODUCTION

Canonical, or β-catenin-dependent, Wnt signaling, which we will refer to as Wnt signaling, is an essential regulator of cell proliferation and differentiation in the vertebrate intestine (Ireland et al., 2004; Korinek et al., 1998; van de Wetering et al., 2002). Inactivating mutations in *APC*, a negative regulator of Wnt signaling, are detected in 80% of hereditary and sporadic forms of colorectal cancer (CRC) (Kinzler et al., 1991; Korinek et al., 1997). Mouse models have shown that inactivation of *Apc* is sufficient to drive intestinal hyperplasia (Andreu et al., 2005; Sansom et al., 2004). Moreover, *Apc* deletion within murine intestinal stem cells (ISCs) results in rapid adenoma formation, suggesting that they can act as cells of origin in CRC (Barker et al., 2009).

Multiple Wnt target genes have been identified in CRC cell lines, mouse models and human tumor samples carrying loss-of-function mutations in *APC* (Holstege and Clevers, 2006; Sansom et al., 2007; Van der Flier et al., 2007). Indeed, 4 days of *Apc* loss in the murine intestine is sufficient to lead to significant dysregulation of hundreds of genes (Sansom et al., 2004). Thus far, very few of these genes have been functionally tested in vivo to directly address their contribution to CRC. The identification of Wnt target genes required for intestinal proliferation in vivo holds great potential for the development of targeted CRC therapies, as well as for regenerative medicine.

[1]Wnt Signaling and Colorectal Cancer Group, [2]*Drosophila* Approaches to Cancer Group, The Beatson Institute for Cancer Research, Garscube Estate, Switchback Road, Glasgow G61 1BD, UK.

*These authors contributed equally to this work
‡Authors for correspondence (j.cordero@beatson.gla.ac.uk; o.sansom@beatson.gla.ac.uk)

Accepted 21 September 2012

Owing to its remarkable resemblance to the vertebrate intestine (Casali and Batlle, 2009), the *Drosophila* adult midgut is emerging as a useful model with which to study intestinal homeostasis, regeneration and abnormal proliferation. Importantly, the fly intestinal epithelium is replenished by its own ISCs (Micchelli and Perrimon, 2006; Ohlstein and Spradling, 2006). *Drosophila* ISCs are randomly scattered along the basal membrane of the intestinal tube and, following division, they give rise to an undifferentiated progenitor, the enteroblast (EB), which differentiates into either the secretory cell lineage represented by the enteroendocrine (ee) cells or the absorptive epithelial cell lineage represented by the enterocytes (ECs). The Wnt signaling pathway shows a significant degree of conservation in the fly intestine. Loss-of-function analyses indicate that Wnt signaling is required for ISC proliferation during homeostasis and regeneration of the *Drosophila* midgut (Lin et al., 2008; Cordero et al., 2012), whereas overexpression of Wg or inactivating mutations in the two *Drosophila Apc* homologs, *Apc1* (*Apc* – FlyBase) and *Apc2*, drive ISC hyperproliferation (Cordero et al., 2009; Lee et al., 2009; Lin et al., 2008). In contrast to the mouse phenotype (Sansom et al., 2004), hyperactivation of Wnt signaling in the *Drosophila* midgut does not affect cell lineage differentiation (Cordero et al., 2009; Lee et al., 2009).

Here we use the posterior adult *Drosophila* midgut to address the molecular mechanisms that mediate ISC hyperproliferation following loss of *Apc* in the intestine. We demonstrate that the Egfr and Jak/Stat signaling pathways are activated in a Myc-dependent manner and are required to drive ISC hyperproliferation in response to *Apc1* loss. Importantly, we provide direct in vivo evidence for paracrine crosstalk between the Egfr and Jak/Stat pathways in *Apc1*-driven intestinal hyperplasia. Finally, our results suggest that the pathways that are ectopically activated in the fly midgut might also be activated in human CRC.

MATERIALS AND METHODS

Fly stocks

The following fly stocks were kindly provided by colleagues: the null alleles *Apc1^{Q8}*, *Apc1^{S176}*, *Apc1^{X1}* and *Apc2^{33}* (Yashi Ahmed, Dartmouth Medical School), *escargot-gal4, UAS-gfp* (Shigeo Hayashi, RIKEN Center for Developmental Biology), *UAS-max-IR* (Peter Gallant, Universität Würzburg), *MyoIA^{ts}>gfp*, *UAS-Upd* and *10×Stat-gfp* (Bruce Edgar, ZMBH, Heidelberg; the latter previously made by Erika Bach, New York University School of Medicine), *upd3.1-lacZ* (Huaqi Jiang, UT Southwestern Medical Center), *MARCM 82B* line (David Bilder, Berkeley), *UAS-DER^{DN}* and *UAS-sSpitz* (Matthew Freeman, MRC LMB, Cambridge). The remainder of the lines used were obtained from the Drosophila Genomics Resource Center (DGRC), Vienna Drosophila RNAi Center (VDRC) and the Bloomington Stock Center. For overexpression of UAS-*wg*, we used Bloomington Stock number 5918. VDRC ID numbers: *UAS-stat-IR* (43866), *UAS-myc-IR* (2947), *UAS-dome-IR* (2612), *UAS-apc1-IR* (1333), *UAS-spitz-IR* (3920).

Fly maintenance

Crosses were maintained at either 18°C or 22°C in standard medium. Animals of the desired genotypes were collected within 48 hours of eclosion, allowed to age for an additional 3-5 days and then switched to the desired temperature. All experiments involving the activation of a transgene under the control of *gal4/gal80^{ts}* were switched from 18°C to 29°C; the rest of the experiments were carried out at 25°C. Animals were kept in incubators with controlled 12-hour light:dark cycles. Flies were changed into new food every 2-3 days. Only posterior midguts from females were analyzed in this study.

Fly genotypes

yw; escargot-gal4, UAS-gfp/+; Apc1^{Q8}FRT82B/+
yw; escargot-gal4, UAS-gfp/+; Apc1^{Q8}FRT82B/Apc1^{Q8}FRT82B
yw; escargot-gal4, UAS-gfp/+; tub-gal80^{ts}/+
yw; escargot-gal4, UAS-gfp/+; tub-gal80^{ts}/UAS-wg
yw; escargot-gal4, UAS-gfp/UAS-arm^{S10}; tub-gal80^{ts}/+
Apc1^{Q8}FRT82B/+
Apc1^{Q8}FRT82B/Apc1^{Q8}FRT82B
tub-gal80^{ts}/+; how-gal4/UAS-gfp
tub-gal80^{ts}/+; how-gal4/UAS-wg
y,w,hsFlp/+; UAS-CD8-gfp, tub-gal4/+; FRT82B, tub-gal80/lacZ FRT82B
y,w,hsFlp/+; UAS-CD8-gfp, tub-gal4/+; FRT82B, tub-gal80/Apc1^{Q8}FRT82B
y,w,hsFlp/+; UAS-CD8-gfp, tub-gal4/+; FRT82B, tub-gal80/Apc2^{33}FRT82B
y,w,hsFlp/+; UAS-CD8-gfp, tub-gal4/+; FRT82B, tub-gal80/Apc1^{Q8}, Apc2^{33}FRT82B
y,w,hsFlp/+; UAS-CD8-gfp, tub-gal4/UAS-max-IR; FRT82B, tub-gal80/lacZ FRT82B
y,w,hsFlp/+; UAS-CD8-gfp, tub-gal4/UAS-max-IR; FRT82B, tub-gal80/ Apc1^{Q8}FRT82B
y,w,hsFlp/+; UAS-CD8-gfp, tub-gal4/UAS-myc-IR; FRT82B, tub-gal80/lacZ FRT82B
y,w,hsFlp/+; UAS-CD8-gfp, tub-gal4/UAS-myc-IR; FRT82B, tub-gal80/ Apc1^{Q8}FRT82B
yw; escargot-gal4, UAS-gfp/+; tub-gal80^{ts}/UAS-Tcf^{DN}
yw; escargot-gal4, UAS-gfp/UAS-arm^{S10}; tub-gal80^{ts}/UAS-Tcf^{DN}
yw; escargot-gal4, UAS-gfp/UAS-myc-IR; tub-gal80^{ts}/+
yw; escargot-gal4, UAS-gfp/UAS-myc-IR; tub-gal80^{ts}/UAS-wg
Canton S (wt)
yw; escargot-gal4, UAS-gfp/UAS-myc-IR,tub-gal80^{ts}; Apc1^{Q8}FRT82B/ Apc1^{Q8}FRT82B
yw; escargot-gal4, UAS-gfp/UAS-myc-IR,tub-gal80^{ts}; Apc1^{Q8}FRT82B/+
UAS-myc-IR,tub-gal80^{ts}/Cyo; Apc1^{Q8}FRT82B/Apc1^{Q8}FRT82B
yw;escargot-gal4,UAS-gfp/UAS-max-IR,tub-gal80^{ts}; Apc1^{Q8}FRT82B/ Apc1^{Q8}FRT82B
yw;escargot-gal4,UAS-gfp/UAS-max-IR,tub-gal80^{ts}; Apc1^{Q8}FRT82B/+
UAS-max-IR,tub-gal80^{ts}/Cyo; Apc1^{Q8}FRT82B/Apc1^{Q8}FRT82B
y,w,hsFlp/+; UAS-CD8-gfp, tub-gal4/UAS-myc-IR,tub-gal80^{ts}; FRT82B, tub-gal80/Apc1^{Q8}FRT82B
y,w,hsFlp/+; UAS-CD8-gfp, tub-gal4/UAS-max-IR,tub-gal80^{ts}; FRT82B, tub-gal80/Apc1^{Q8}FRT82B
upd3.1-lacZ/+; Apc1^{Q8}FRT82B/+
upd3.1-lacZ/+; Apc1^{Q8}FRT82B/Apc1^{Q8}FRT82B
yw; escargot-gal4, UAS-gfp/upd3.1-lacZ; tub-gal80^{ts}/+
yw; escargot-gal4, UAS-gfp/upd3.1-lacZ; tub-gal80^{ts}/UAS-wg
y,w,hsFlp/+; UAS-CD8-gfp, tub-gal4/upd3.1-lacZ; FRT82B, tub-gal80/ Apc1^{Q8}FRT82B
10×Stat-gfp/+; Apc1^{Q8}FRT82B/+
10×Stat-gfp/+; Apc1^{Q8}FRT82B/Apc1^{Q8}FRT82B
yy,w,hsFlp/+; UAS-CD8-gfp,tub-gal4/UAS-stat-IR; FRT82B, tub-gal80/ Apc1^{Q8}FRT82B
y,w,hsFlp/+; UAS-CD8-gfp, tub-gal4/UAS-dome-IR; FRT82B, tub-gal80/ Apc1^{Q8}FRT82B
yw; escargot-gal4, UAS-gfp/dome-IR; tub-gal80^{ts}/+
yw; escargot-gal4, UAS-gfp/UAS-stat-IR; tub-gal80^{ts}/+
yw; escargot-gal4, UAS-gfp/UAS-dome-IR; tub-gal80^{ts}/UAS-wg
yw; escargot-gal4, UAS-gfp/UAS-stat-IR; tub-gal80^{ts}/UAS-wg
yw; escargot-gal4, UAS-gfp/UAS-upd; tub-gal80^{ts}/+
yw; escargot-gal4, UAS-gfp/UAS-upd,UAS-myc-IR; tub-gal80^{ts}/+
yw; escargot-gal4, UAS-gfp/upd3.1-lacZ; tub-gal80^{ts}/UAS-sSpitz
yw; escargot-gal4, UAS-gfp/UAS-Apc1-IR; tub-gal80^{ts}/UAS-Apc1-IR
yw; escargot-gal4, UAS-gfp/+; tub-gal80^{ts}/UAS-spi-IR
yw; escargot-gal4, UAS-gfp/UAS-Apc1-IR; UAS-spi-IR/UAS-Apc1-IR
MyoIA-gal4/+; UAS-gfp, tub-gal80^{ts}/+
MyoIA-gal4/+; UAS-gfp, tub-gal80^{ts}/UAS-wg
MyoIA-gal4/UAS-DER^{DN}; UAS-gfp, tub-gal80^{ts}/+
MyoIA-gal4/UAS-DER^{DN}; UAS-gfp, tub-gal80^{ts}/UAS-wg
spi-gal4^{NP0261}/UAS-egfp
vn-lacZ/Tm3
y,w,hsFlp/+; UAS-CD8-gfp,tub-gal4/UAS-DER^{DN};FRT82B, tub-gal80/ Apc1^{Q8}FRT82B
yw; escargot-gal4, UAS-gfp/+; tub-gal80^{ts}/UAS-myc
yw; escargot-gal4, UAS-gfp/upd3.1-lacZ; tub-gal80^{ts}/UAS-myc
UAS-dicer2/+; escargot-gal4, UAS-gfp/+; tub-gal80^{ts}/UAS-Apc1-IR
UAS-dicer2/+; escargot-gal4, UAS-gfp/UAS-myc-IR; tub-gal80^{ts}/UAS-Apc1-IR

Histology and tissue analysis

For immunofluorescence, tissues were dissected and stained as described (Cordero et al., 2012). Primary antibodies were: chicken anti-GFP, 1:4000 (Abcam); mouse anti-Delta, 1:20 [Developmental Studies Hybridoma Bank (DSHB)]; mouse anti-Prospero, 1:20 (DSHB); mouse anti-Armadillo, 1:3 (DSHB); rabbit anti-pH3 S10 and S28, 1:100 (Cell Signaling); guinea pig anti-Myc, 1:100 and pre-absorbed (from G. Morata, SIC-UAM, Madrid); rabbit anti-β-gal, 1:1000 (Cappel); rabbit anti-Pdm1 (Nubbin), 1:500 (from W. Chia, King's College, London). Secondary antibodies were: Alexa 488, 1:200 and Alexa 594, 1:100 (Invitrogen); Cy5, 1:50 (Jackson Laboratories). Confocal images were captured using a Zeiss 710 confocal microscope and processed with Adobe Photoshop CS to adjust brightness and contrast. Images represent a maximum intensity projection of *z*-stacks.

For immunohistochemistry, fly intestines were dissected and fixed in 10% formalin and then paraffin embedded to allow sectioning and Hematoxylin and Eosin (H+E) staining.

Clonal analysis

Recombinant clones were generated using the MARCM technique as previously described (Lee and Luo, 2001). Crosses were maintained at 22°C. Then, 3- to 5-day-old adults of the desired genotypes were selected and subject to three 30-minute heat shocks at 37°C in 1 day. Flies were then incubated at 25°C and their guts dissected for analysis 2 weeks after clonal induction. ISC proliferation was scored by the number of cells per clone and percentage of clones with pH3^{+} cells.

Regression of *Apc1^{Q8}* phenotypes

Whole gut

We analyzed the midgut of animals carrying the following alleles and transgenes: (1) *esg>gfp; Apc1$^{Q8/+}$* (*Apc1$^{Q8/+}$*); (2) *esg>gfp; Apc1^{Q8}* (*Apc1^{Q8}*); (3) *Apc1^{Q8}* carrying the *esg>gfp* driver in combination with

UAS-myc-IR^{ts} or *UAS-max-IR^{ts}* transgenes (*Apc1^{Q8}* + *myc-IR^{ts}* and *Apc1^{Q8}* + *max-IR^{ts}*, respectively). Adults were kept at room temperature for 5 days, after which their midguts were analyzed or transferred to 29°C for 7 days to allow RNAi expression (*Apc1^{Q8}* + *myc-IR^{ts}* and *Apc1^{Q8}* + *max-IR^{ts}*). Midguts were dissected and the total number of pH3^{+} cells per posterior midgut was quantified. See Fig. 3.

MARCM clones

Clones carrying the following alleles and transgenes were induced and allowed to develop at 22°C for 14 days: (1) control (*lacZ*); (2) *Apc1^{Q8}*; (3) *UAS-myc-IR^{ts}; Apc1^{Q8}* (*myc-IR*); (4) *UAS-max-IR^{ts}; Apc1^{Q8}* (*max-IR*). After the first 14 days, all flies were switched to 29°C and midguts were dissected after 1 day (15-day-old clones; 15d), 7 days (21-day-old clones; 21d) and 14 days (28-day-old clones; 28d) of incubation at 29°C. The latter incubation was only performed for *UAS-myc-IR^{ts}; Apc1^{Q8}* and *UAS-max-IR^{ts}; Apc1^{Q8}* MARCM clones. ISC proliferation was scored by the number of cells per clone and percentage of clones with pH3^{+} cells. See supplementary material Fig. S3.

Lifespan studies

For each study, 30-50 flies were used. Flies were collected within 48 hours after eclosion and kept at a density of 20 flies per vial at 22°C or 29°C in a controlled 12-hour light:dark cycle. Every 2-3 days, vials were changed and the number of dead flies was counted, from which mean and maximum lifespan (MLS, the last 10% of surviving flies) were calculated. Prism (GraphPad) software was utilized to build survival curves analyzed using the Kaplan Meier log-rank test.

RNA quantification

TRIZOL (Invitrogen) was used to extract total RNA from 6-10 midguts per biological replicate. cDNA synthesis from three biological replicates was performed using the High-Capacity cDNA Reverse Transcription Kit (Applied Biosystems). MAXIMA SYBR Green Master Mix (Fermentas) was used for quantitative (q) PCR. Data were extracted and analyzed using Applied Biosystems 7500 software version 2.0 and Prism. Data are presented as the mean fold change with standard error. Primers are listed in supplementary material Table S1.

Quantifications and statistics

In each experiment, 5-15 midguts were analyzed. Clonal sizes were quantified as the total number of cells per clone (scored by DAPI staining). ISC proliferation was quantified as the total number of pH3^{+} cells per posterior midgut. Different cell lineages in control and *Apc1^{Q8}* MARCM clones were quantified as percentage of ECs, ee or ISCs (scored by nuclear size, Prospero or Delta staining, respectively) among the total number of cells per clone (scored by DAPI). Quantification of ISCs was also represented by the number of Delta^{+} cells per clone. For the quantification of Delta^{+} cells in whole *Apc1$^{Q8/+}$* and *Apc1^{Q8}* midguts, we counted the total number of Delta^{+} cells within a consistent region of the posterior midgut, which was imaged with a 40× lens and comprised a field of 0.04 mm^{2}. The percentage of Myc^{+}/*esg>gfp*$^{+}$ cells in posterior midguts was calculated as the number of *esg>gfp*$^{+}$ cells that showed Myc staining over the total number of *esg>gfp*$^{+}$ cells within a consistent region of the posterior midgut imaged as above. Results are presented in graphs created by Prism 5. We used Student's *t*-test or one-way ANOVA with Bonferroni's multiple comparison test for statistical analysis.

Mouse and human tissue staining

All experiments were performed following UK Home Office guidelines. Alleles and induction protocols used were as previously described (Sansom et al., 2007; Ireland et al., 2004; Barker et al., 2007).

We performed standard immunohistochemistry of formalin-fixed intestinal sections. Primary antibodies were c-Myc (1:100; Santa Cruz sc-40) and p-Stat3 (1:1000; Santa Cruz sc-7993-R).

Colon carcinoma tissue arrays (CO804a, Biomax.us) were stained with the indicated primary antibodies and individual cores scored based on the percentage of each core with a staining intensity of 0, 1, 2 or 3. Staining intensities were analyzed using the Spearman's rank correlation coefficient.

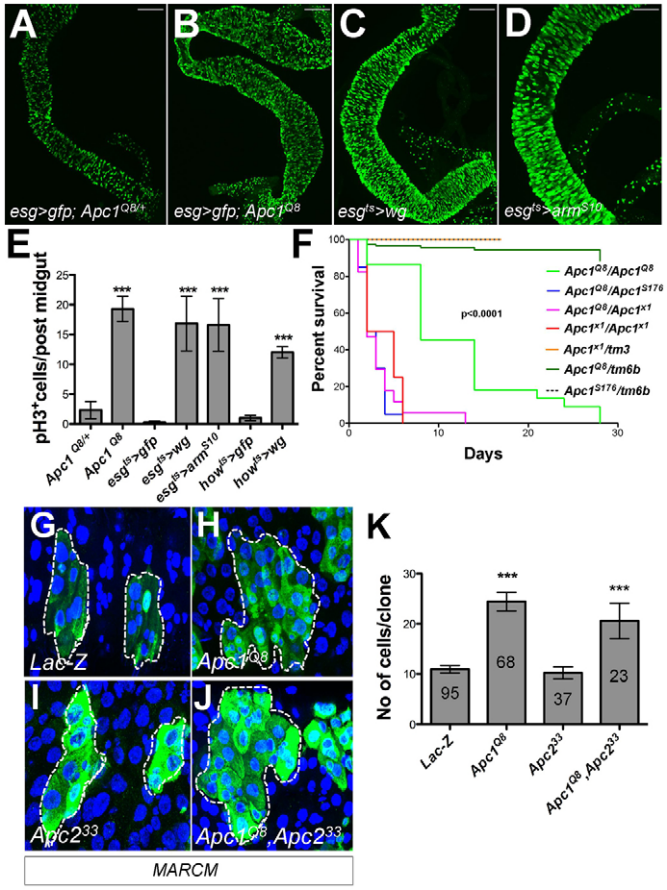

Fig. 1. *Apc1* but not *Apc2* regulates ISC proliferation in the *Drosophila* midgut. (**A**,**B**) Posterior midguts from 5-day-old *Apc1$^{Q8/+}$* (A) and *Apc1^{Q8}* (B) animals carrying the *esg-gal4; UAS-gfp* (*esg>gfp*) driver (green) in the background. (**C**,**D**) Midguts overexpressing *wg* (*esg^{ts}>wg*; C) or *arm^{S10}* (activated form; *esg^{ts}>arm^{S10}*; D) for 14 days under the temperature-sensitive *esg>gfp* driver (*esg^{ts}>gfp*). (B-D) Note the increase in *esg*$^{+}$ cells and tissue hyperplasia. (**E**) Quantification of intestinal stem cell (ISC) proliferation in midguts as in A-D and after Wg overexpression in the visceral muscle (*how^{ts}>wg*) for 14 days, as represented by the number of pH3^{+} cells in the posterior midgut. (**F**) Survival analysis of *Apc1^{Q8}*, *Apc1^{S176}* and *Apc1^{x1}* flies. *P*=0.0001, log-rank Mantel-Cox test. (**G-J**) 14-day-old control (*lacZ*) (G), *Apc1^{Q8}* (H), *Apc2^{33}* (I) and *Apc1^{Q8}, Apc2^{33}* (J) MARCM clones (GFP^{+} and outlined by dashed line). (**K**) Quantification of the number of cells per clone. Numbers within bars indicate total number of clones scored. ***P<0.0001, one-way ANOVA with Bonferroni's multiple comparison test. Error bars indicate s.e.m. Unless otherwise noted, DAPI (blue) was used to stain nuclei. Scale bars: 50 μm.

RESULTS

Apc1 but not *Apc2* is required for ISC hyperproliferation in the *Drosophila* adult midgut

Drosophila Apc1 and *Apc2* are redundant during development (Ahmed et al., 2002). Nevertheless, both genes have been shown to independently regulate stem cell divisions in the male *Drosophila* germ line (Yamashita et al., 2003).

Concomitant knockdown of the two *Drosophila Apc* homologs in progenitor cells results in ISC hyperproliferation (Cordero et al., 2009; Lee et al., 2009) within the *Drosophila* adult midgut. We therefore examined whether independent roles of *Apc1* and *Apc2* can be distinguished in the regulation of ISC proliferation. We

examined the posterior midguts from animals carrying the null allele *Apc1*^{Q8} (Ahmed et al., 1998) in combination with the stem/progenitor cell driver *escargot-gal4, UAS-gfp* (*esg>gfp*) (Micchelli and Perrimon, 2006). We will refer to the *Apc1*^{Q8} allele as *Apc1*. We observed that the midguts of *Apc1* animals displayed a hyperplastic phenotype, which was characterized by ISC hyperproliferation as demonstrated by a significant increase in phosphorylated Histone H3-positive (pH3^{+}) and *esg>gfp*$^{+}$ cells (Fig. 1A,B,E). This phenotype was comparable to that resulting from overexpression of Wg or the activated form of β-catenin/Armadillo (Arm^{S10}) in stem/progenitor cells under the inducible *escargot-gal4, UAS-gfp; tub-gal80*^{ts} driver (*esg*^{ts}*>wg* and *esg*^{ts}*>arm*^{S10}, respectively) (Fig. 1C-E; supplementary material Fig. S2G,J,L). Furthermore, whole animals homozygous for loss-of-function alleles of *Apc1* displayed a significantly decreased lifespan when compared with heterozygote controls (Fig. 1F). No intestinal hyperproliferation or decrease in lifespan was observed in animals lacking *Apc2* only (data not shown).

To confirm the role of *Apc1* in ISC proliferation and to test whether there was any contribution from *Apc2*, we created MARCM clones (Lee and Luo, 2001) of cells deficient for *Apc1* or *Apc2* only and compared them with *Apc1, Apc2* double-mutant clones (Fig. 1G-J) (Cordero et al., 2009; Lee et al., 2009). Consistent with the whole mutant phenotype, intestinal *Apc1* clones had more cells than control (*lacZ*) clones (Fig. 1G,H,K). Importantly, no difference was observed between *Apc2* and control clones (Fig. 1G,I,K). Furthermore, *Apc1* clones showed no significant difference in size when compared with *Apc1, Apc2* double-mutant clones (Fig. 1H,J,K). As previously reported in *Apc1, Apc2* double mutants (Cordero et al., 2009; Lee et al., 2009), loss of *Apc1* in the *Drosophila* midgut resulted in increased ISC proliferation with no major differentiation defects (supplementary material Fig. S1). We did, however, note that MARCM *Apc1* clones had a slight increase in the percentage of ECs and increased numbers of Delta^{+} ISCs (Ohlstein and Spradling, 2007), which was proportional to the increase in the total number of cells (supplementary material Fig. S1). These phenotypes mimic the accumulation of ECs due to impaired sloughing off and upregulation of Lgr5^{+} ISCs observed in the *Apc* mouse intestine (Barker et al., 2009; Sansom et al., 2004).

Taken together, these results indicate that loss of *Apc1* is responsible for ISC hyperproliferation in *Apc1, Apc2* MARCM clones in the *Drosophila* midgut (Cordero et al., 2009; Lee et al., 2009). This phenotype strongly resembles that of the mammalian intestine (Sansom et al., 2004), indicating a significant degree of evolutionary conservation in the biology of this tissue. Therefore, the adult *Drosophila* midgut is a useful system for the identification of key downstream signaling events following *Apc1* loss.

Myc is upregulated and required for ISC hyperproliferation downstream of Wg signaling

Myc proteins are well-known proto-oncogenes and general, although not universal, regulators of normal growth and proliferation (Johnston et al., 1999; Trumpp et al., 2001). Myc dysregulation is observed in a wide range of human tumors (Vita and Henriksson, 2006). In the mouse, c-Myc is an essential mediator of the *Apc* phenotypes in the intestine (Sansom et al., 2007) but not in the liver (Reed et al., 2008). *Drosophila* Myc [also known as dMyc or Diminutive (Dm) – FlyBase] acts downstream of Wg during epithelial regeneration in the larval wing disc (Smith-Bolton et al., 2009), although it is not required for cells with high Wnt signaling to act as supercompetitors (Vincent et al., 2011).

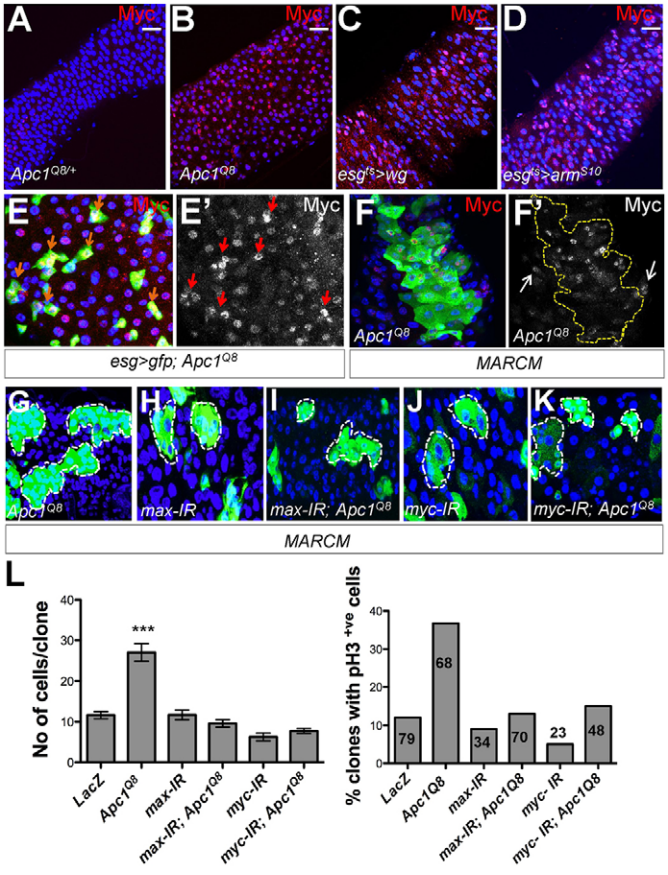

Fig. 2. Myc upregulation mediates Wnt-dependent hyperproliferation in the *Drosophila* midgut.
(**A-F′**) Immunofluorescence for Myc (red or white) in posterior midguts. (A,B) Tissue from 5-day-old whole *Apc1*$^{Q8/+}$ (A) or *Apc1*^{Q8} (B) animals. (C,D) *esg*^{ts}*>wg* (C) or *esg*^{ts}*>arm*^{S10} (D) midguts after 14 days of transgene overexpression. (E,E′) Midguts from 5-day-old whole *Apc1*^{Q8} animals combined with *esg>gfp* (green; E) to label progenitor ISCs/enteroblasts (EBs). Myc levels were clearly elevated within the *esg*$^{+}$ cells (arrows). (F,F′) Myc staining in 14-day-old MARCM *Apc1*^{Q8} clone (GFP^{+} or outlined by dashed line). Note Myc upregulation outside the clone (arrows). (**G-K**) 14-day-old MARCM clones of the indicated genotypes stained with anti-GFP (green and outlined by dashed line). (**L**) Quantification of the number of cells per clone (left) and percentage of clones with pH3^{+} cells (right) in MARCM clones as in G-K. Numbers inside bars indicate the total number of clones scored. ***P<0.0001, one-way ANOVA with Bonferroni's multiple comparison test. Error bars indicate s.e.m. Scale bars: 20 μm.

Therefore, the interactions between Wnt signaling and Myc seem to be highly context dependent.

We tested whether there was a role for Myc in Wnt-driven hyperplasia in the *Drosophila* midgut. First, we examined the levels of Myc expression in *esg*^{ts}*>wg*, *esg*^{ts}*>arm*^{S10} and *Apc1* intestines and observed that Myc protein was significantly upregulated in all cases compared with wild-type tissues (Fig. 2A-D; supplementary material Fig. S2A,B′). Importantly, the ISC-EB cell population, labeled by *esg-gfp*, displayed the highest levels of Myc (Fig. 2E,E′; supplementary material Fig. S2A-B′). Previous work shows that *Apc*-driven ISC proliferation in the *Drosophila* midgut involves the Arm (β-catenin) co-factor Pangolin (Tcf) (Lee et al., 2009). Consistently, Myc upregulation was dependent on Pangolin (supplementary material Fig. S2C-D′). Myc staining of *Apc1*

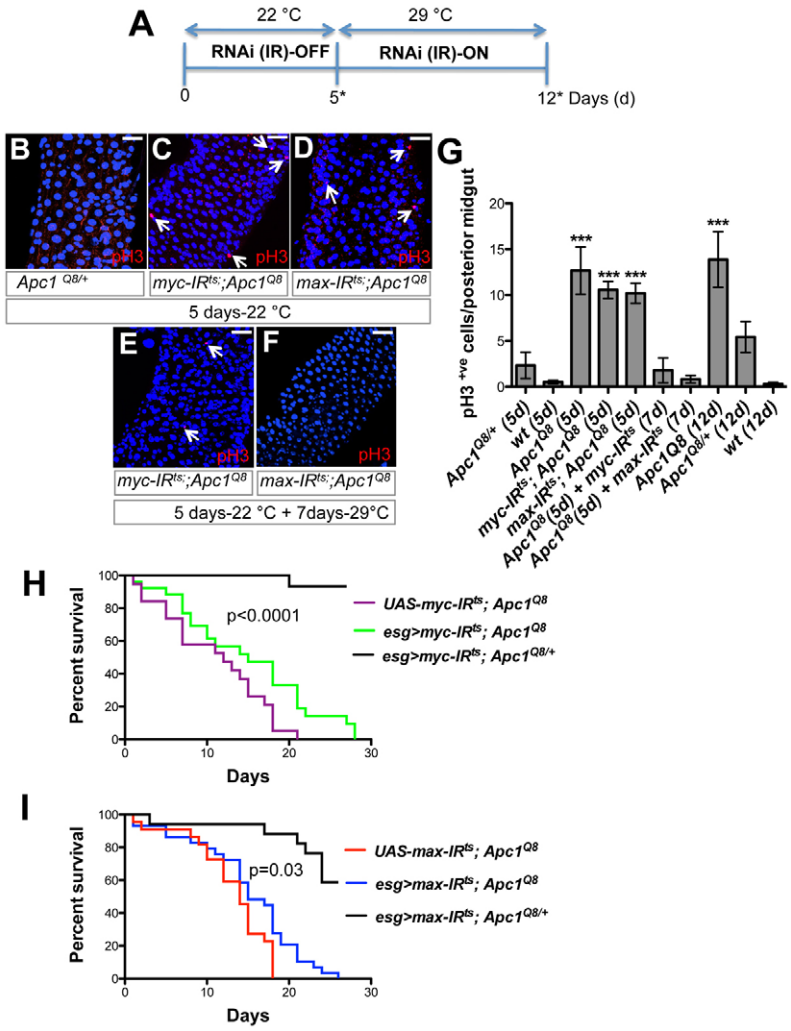

Fig. 3. Myc and Max depletion regresses established *Apc1* intestinal hyperproliferation. (**A**) The experimental setup. Flies were maintained at 22°C for 5 days after eclosion followed by incubation at 29°C for 7 days to allow RNAi (*myc-IR*^{ts} and *max-IR*^{ts}) expression in progenitor *esg*$^{+}$ cells. Cohorts were analyzed at the time points indicated by asterisks. (**B-F**) Posterior midguts from 5-day-old whole *Apc1*$^{Q8/+}$ (B), *esg>myc-IR*^{ts}*; Apc1*^{Q8} (C) and *esg>max-IR*^{ts}*; Apc1*^{Q8} (D) animals incubated at 22°C (RNAi 'off'; B-D) or *esg>myc-IR*^{ts}*; Apc1*^{Q8} (E) and *esg>max-IR*^{ts}*; Apc1*^{Q8} (F) animals switched to 29°C for an additional 7 days (RNAi 'on'; E,F). Arrows point to pH3^{+} cells (red). (**G**) Quantification of the number of pH3^{+} cells per posterior midgut before (5d, 5 days at 22°C) and after *myc-IR* or *max-IR* expression (5d + 7d, 5 days at 22°C followed by 7 days at 29°C). Proliferation was also scored in midguts from wild-type, *Apc1*$^{Q8/+}$ and *Apc1*^{Q8} animals kept at 22°C (12d). ***P<0.0001, one-way ANOVA with Bonferroni's multiple comparison test. Error bars indicate s.e.m. (**H**,**I**) Survival analysis of animals of the indicated genotypes. Knockdown of *myc* (H) or *Max* (I) in ISCs improved total survival of *Apc1*^{Q8} animals (log-rank Mantel-Cox test). Scale bars: 20 μm.

MARCM clones revealed autonomous as well as non-autonomous upregulation of Myc outside the clones (Fig. 2F,F′, arrows).

In order to functionally test the importance of Myc upregulation in response to *Apc1* loss, we used the MARCM system to target RNA interference (RNAi) for *myc* (*myc-IR*) or its transcriptional partner *Max* (*max-IR*) (Steiger et al., 2008) within *Apc1* mutant clones. *myc-IR* and *max-IR* overexpression completely suppressed hyperproliferation of *Apc1* MARCM clones (Fig. 2G-L). Even though clones of *myc-IR* had reduced ISC proliferation when compared with *lacZ* control clones (Fig. 2J,L), overexpression of either *myc-IR* or *max-IR* in *Apc1* clones resulted in clonal sizes and proliferation levels comparable to those of the RNAi transgenes alone (Fig. 2L). Furthermore, knockdown of *myc* also suppressed hyperproliferation induced by Wg overexpression (supplementary material Fig. S2E-L). Together, these results demonstrate that Myc has a conserved role in mediating *Apc1*-driven hyperproliferation in the intestine.

myc proto-oncogene addiction in *Apc1*-driven hyperproliferation

Oncogene addiction is a process in cancer biology through which tumors may become dependent on certain pathways not just for proliferation and growth but also for maintenance and survival (Felsher, 2008). Studies of oncogene addiction have generally been performed by overexpression of exogenous transgenes (e.g. *Kras* and *Myc*), which are then switched off within the tumors that they initiated, leading to tumor regression (Felsher and Bishop, 1999). A more relevant question for human tumorigenesis is whether switching off endogenous levels of proteins driven by an oncogenic or tumor suppressor mutation will also cause tumor regression. Recent studies have shown that transient overexpression of the dominant-negative Myc protein 'Omo-Myc', which is thought to prevent Myc/Max dimerization, can cause tumor regression in established lung adenomas driven by *KRAS* mutation (Soucek et al., 2008). We have previously shown that Apc deficiency in the mouse intestine requires Myc at the onset of hyperplasia (Athineos and Sansom, 2010; Sansom et al., 2007). Nevertheless, no studies have shown whether there is a sustained requirement for Myc in this context.

We tested whether the *Apc1*-driven hyperproliferation in the adult *Drosophila* midgut is dependent on Myc once established. We first used *Apc1* whole mutant animals to assess whether downregulation of *myc* and *Max* within the *esg*$^{+}$ cell population could affect hyperproliferation across the entire intestinal epithelium. We created temperature-sensitive *myc* and *Max* RNAi (*tub-gal80*^{ts}*, UAS-myc-IR* and *tub-gal80*^{ts}*, UAS-max-IR*, respectively), which we placed in the background of whole *Apc1* animals carrying the *esg>gfp* driver (Fig. 3). Animals of the desired genotype were allowed to age at the non-permissive temperature for 5 days, following which we 'turned on' the RNAi

for an additional 7 days (Fig. 3A). Before turning on the RNAi, *Apc1* midguts displayed the expected hyperproliferative phenotype (Fig. 3C,D,G). After 7 days of RNAi for either *myc* or *Max*, hyperproliferation was almost completely reverted (Fig. 3E-G). A similar outcome was observed in the context of MARCM *Apc1* clones (supplementary material Fig. S3). Taken together, these experiments indicate that the *Apc1* hyperproliferative phenotype not only requires Myc for its establishment but also for its maintenance. Strikingly, *myc* or *Max* knockdown in *esg*$^{+}$ cells enhanced total survival from whole *Apc1* mutant animals (Fig. 3H,I).

Loss of *Apc1* leads to Jak/Stat pathway activation

The non-cell-autonomous upregulation of Myc in MARCM clones of *Apc1* (Fig. 2F,F′) suggested the production of secreted factors within *Apc1* mutant tissues, which might contribute to hyperproliferation of the adult *Drosophila* midgut. We took a candidate approach and performed RT-qPCR from *Apc1* whole midguts to look at levels of known regulators of ISC proliferation, which may be secreted (Biteau and Jasper, 2011; Jiang et al., 2009; Karpowicz et al., 2010; Ren et al., 2010; Shaw et al., 2010; Buchon et al., 2009; Jiang et al., 2011).

Jak/Stat signaling is required for *Drosophila* intestinal homeostasis and regeneration. Overexpression of the ligand Upd is sufficient to drive ISC hyperproliferation (Beebe et al., 2010; Buchon et al., 2009; Jiang et al., 2009; Lin et al., 2010). Additionally, Jak/Stat mediates hyperproliferation induced by loss of the tumor suppressor Hippo or hyperactivation of Egfr signaling (Biteau and Jasper, 2011; Jiang et al., 2011; Jiang et al., 2009; Karpowicz et al., 2010; Ren et al., 2010; Shaw et al., 2010).

RT-qPCR of whole *Apc1* and *esg*^{ts}*>wg* midguts indicated significant upregulation of the interleukin-like ligands *upd2* and *upd3*, as well as the downstream target of the pathway *Socs36E* (Fig. 4A). As *upd3* showed the highest upregulation, we investigated its tissue expression domain using a *lacZ* reporter (Jiang et al., 2009). This showed that, either whole tissue loss of *Apc1* or overexpression of Wg in ISCs resulted in activation of *upd3-lacZ* almost exclusively in ECs. These are characterized by their large nuclei, lack of Delta and Prospero staining and absence of *esg>gfp* (Fig. 4B-E′; supplementary material Fig. S4). In a similar scenario to Myc upregulation (Fig. 2F,F′), MARCM clones of *Apc1* revealed non-autonomous activation of *upd3* expression (Fig. 4F-F″, arrows). A transgenic reporter of Jak/Stat pathway activation, *Stat-GFP* (Bach et al., 2007), showed that loss of *Apc1* in the midgut led to upregulation in Jak/Stat pathway activity primarily within stem/progenitor cells (Fig. 4G-J). Together, these data suggest that, in the context of *Apc1* loss, Upd3 is secreted from ECs and activates Jak/Stat signaling in ISCs.

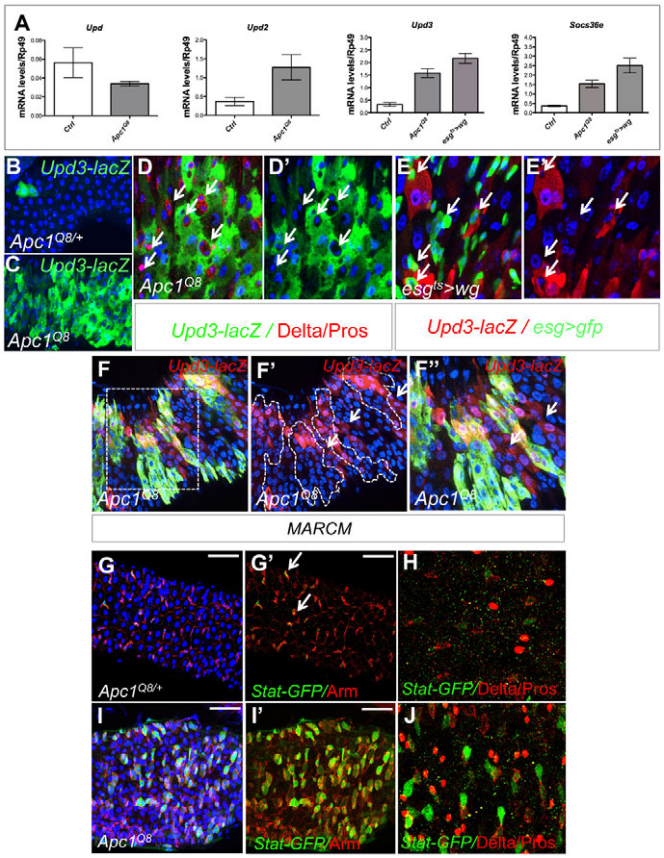

Fig. 4. The Jak/Stat pathway is upregulated downstream of *Apc1* loss. (**A**) RT-qPCR for *upd* (*upd1, outstretched*), *upd2*, *upd3* and *Socs36e* in whole *Apc1*^{Q8} and *esg*^{ts}*>wg* intestines. Error bars indicate s.e.m. (**B-D′**) Posterior midguts from 5-day-old whole *Apc1*$^{Q8/+}$ (control; B) or *Apc1*^{Q8} (C-D′) carrying the *upd3-lacZ* reporter (green). (D) Midguts were immunostained for Delta and Prospero (red) to label ISCs and enteroendocrine (ee) cells, respectively. Arrows (D,D′) point to Delta^{+} or Prospero^{+} cells, which did not express *upd3-lacZ*. (**E**,**E′**) *upd3-lacZ* reporter expression (red) in *esg*^{ts}*>wg* posterior midguts following 14 days of transgene overexpression. Arrows point to ISCs/EBs labeled with *esg>gfp* (green). (D-E′) In both genetic contexts, *upd3* was almost exclusively upregulated in ECs, which are characterized by their large nuclei and lack of expression of Delta, Prospero and *esg>gfp*. (**F-F″**) *upd3-lacZ* reporter (red) in the background of 14-day-old *Apc1*^{Q8} MARCM clones (GFP^{+} or outlined with dashed line). Arrows point to areas of *upd3* upregulation outside the clones. (F′,F″) Magnification of boxed area in F. (**G-J**) 5-day-old whole *Apc1*$^{Q8/+}$ (G-H) or *Apc1*^{Q8} (I-J) posterior midguts carrying a GFP reporter for Jak/Stat pathway activity (*Stat-GFP*; green) and immunostained for Arm (G′,I′; red) or Delta and Prospero (H,J; red). Arrows (G′) point to Arm-rich ISCs showing low basal levels of *Stat-GFP*. Complementary to *upd3*, *Stat* activation was mostly upregulated within ISCs and EBs. Scale bars: 50 μm.

Jak/Stat mediates *Apc1*-dependent hyperproliferation

To test the functional relevance of Jak/Stat signaling activation upon *Apc1* loss we used the MARCM system to drive RNAi for *Stat* (*stat-IR; Apc1*) or the receptor *domeless* (*dome-IR; Apc1*) within clones of *Apc1* (Fig. 5A-C). *Stat* or *dome* knockdown on its own does not prevent ISC proliferation but affects differentiation (Beebe et al., 2010; Buchon et al., 2009; Jiang et al., 2009). Remarkably, loss of either component of the Jak/Stat signaling pathway significantly suppressed the hyperproliferative phenotype of *Apc1* clones (Fig. 5A-D), as well as that of Wg-overexpressing midguts (Fig. 5E-J). Therefore, Jak/Stat signaling upregulation is essential to drive ISC hyperproliferation by high Wg signaling in the *Drosophila* midgut.

We next investigated the epistatic relationship between *Apc1* and Jak/Stat signaling in the adult *Drosophila* midgut. First, we looked at Jak/Stat signaling pathway activation in *Apc1* intestines with *myc* knockdown. RT-PCR of whole midguts indicated that activation of Jak/Stat signaling in *Apc1* midguts is almost entirely dependent on Myc activation in ISCs (Fig. 6A). We next examined Myc levels in *stat-IR; Apc1* and *dome-IR; Apc1* MARCM clones (Fig. 6B-D′).

Myc upregulation upon *Apc1* loss (Fig. 6B,B′) was diminished in *dome-IR; Apc1* clones (Fig. 6C,C′) but still significantly upregulated in *stat-IR; Apc1* clones (Fig. 6D-D′). These results were confirmed upon *dome* and *Stat* knockdown from *wg*-overexpressing midguts (Fig. 6E-H). Moreover, *upd1* overexpression induced upregulation of Myc (Fig. 6I-J′), which might at least partly explain the non-autonomous activation of Myc in *Apc1* clones (Fig. 2). Upregulation of Myc was required for Upd-dependent ISC hyperproliferation (Fig. 6K). Together, these results suggest the presence of a positive-feedback crosstalk between Myc and Jak/Stat activation in response to *Apc1* loss in the *Drosophila* midgut.

Egfr signaling mediates Wnt/Myc and Jak/Stat signaling crosstalk

The non-autonomous activation of *upd3* in ECs in response to high levels of Wnt/Myc signaling in ISCs (Figs 4, 5) suggested the existence of paracrine signaling between ISCs and ECs. Crosstalk between Jak/Stat and Egfr/Ras/MAPK signaling mediates ISC proliferation during homeostasis and regeneration of the adult *Drosophila* midgut. Overexpression of EGF-like ligands leads to upregulation of *upd1-3* and subsequent Jak/Stat pathway activation. Conversely, ectopic *upd1* overexpression results in upregulation of EGF-like ligands and activation of Egfr signaling (Biteau and Jasper, 2011; Buchon et al., 2010; Jiang et al., 2011). Therefore, we hypothesized that the Egfr pathway could provide a link between Wnt/Myc and Jak/Stat signaling.

RT-qPCR of whole *Apc1* and *esg^{ts}>wg* midguts showed selective upregulation of the EGF-like ligands *spitz* and *vein* (Fig. 7A; supplementary material Fig. S5A). Of these, only the upregulation of *spitz* was dependent on Myc expression in ISCs (Fig. 7A). Like Myc, *spitz* is normally expressed in ISCs/EBs (supplementary material Fig. S5B-C′), whereas *vein* is predominantly expressed in the visceral muscle (supplementary material Fig. S5D,D′) (Buchon et al., 2010; Biteau and Jasper, 2011; Jiang et al., 2011). This suggested that Spitz might be functionally required downstream of Myc, causing the paracrine activation of Upd3. To test this, we overexpressed a secreted form of Spitz in progenitor cells (*esg^{ts}>sSpitz*), which led to *upd3* upregulation in ECs (Fig. 7B; supplementary material Fig. S5E,E′) in a similar fashion to *esg^{ts}>wg* midguts (Fig. 4). Given that Jak/Stat signaling is absolutely required for *Apc1*-dependent ISC proliferation, if the activation of Spitz is required for *upd3* expression then it should also be necessary for ISC hyperproliferation in this context. We made use of RNAi for *spitz* (*spitz-IR*) (Buchon et al., 2010) and *Apc1* (*Apc1-IR*) (Cordero et al., 2009) to test whether Spitz from ISCs/EBs is required for *Apc1*-dependent ISC hyperproliferation (Fig. 7D,G). Owing to the chromosomal location of the available transgenes, we could not test this hypothesis in a MARCM setting. Consistent with the *Apc1* loss-of-function phenotype, overexpression of *Apc1-IR* in progenitor cells (*esg^{ts}>Apc1-IR*) resulted in ISC hyperproliferation (Fig. 7D,G), which was dependent on Myc upregulation (supplementary material Fig. S8). Importantly, concomitant knockdown of *spitz* and *Apc1* (*esg^{ts}>spitz-IR; Apc1-IR*) completely suppressed ISC hyperproliferation from *esg^{ts}>Apc1-IR* midguts (Fig. 7F,G). These results suggest that Egfr activation by Spitz mediates ISC hyperproliferation in response to *Apc1* deficiency in the midgut. Consistently, overexpression of a dominant-negative form of Egfr in the background of *Apc1* MARCM clones (*DER^{DN};Apc1^{Q8}*) completely suppressed the phenotype of *Apc1* MARCM clones (supplementary material Fig. S5L).

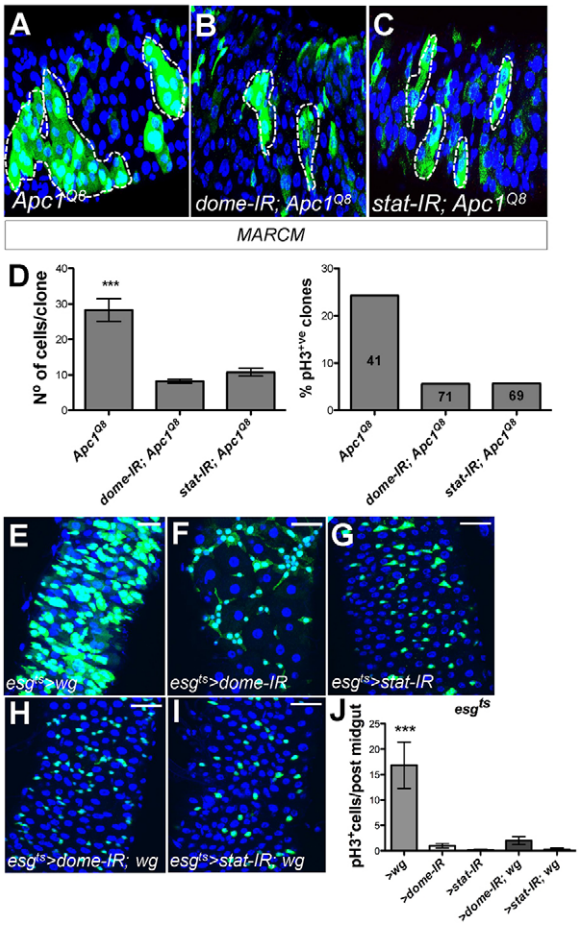

Fig. 5. Jak/Stat pathway activation is required for ISC hyperproliferation in response to high Wnt signaling. (**A-C**) 14-day-old MARCM clones (GFP^{+} and outlined with dashed line) of *Apc1^{Q8}* (A) or combined with RNAi for *domeless* (*dome-IR; Apc1^{Q8}*) (B) or *Stat* (*stat-IR; Apc1^{Q8}*) (C). (**D**) Quantification of the number of cells per clone (left) and percentage of clones with pH3^{+} cells (right). Numbers inside bars indicate the number of clones scored. (**E-I**) Posterior midguts overexpressing *wg* (E), *dome-IR* (F), *stat-IR* (G), *dome-IR* and *wg* (*dome-IR; wg*) (H) or *stat-IR* and *wg* (*stat-IR; wg*) (I) in progenitor cells for 14 days and stained with anti-GFP (green). (**J**) Quantification of ISC proliferation from E-I, as represented by the number of pH3^{+} cells in the posterior midgut. ***P<0.0001, one-way ANOVA with Bonferroni's multiple comparison test. Error bars indicate s.e.m. Scale bars: 20 μm.

We next designed a strategy to directly address the role of Egfr signaling in the upregulation of *upd3* in ECs. Egfr activation in ECs has been shown to regulate gut remodeling in response to bacterial infection (Buchon et al., 2010). We tested whether preventing Egfr function in ECs affects *upd3* upregulation in the same cells and ISC proliferation in the context of high Wnt signaling. As in the case of other secreted ligands (Jiang et al., 2011), ectopic overexpression of Wg in different cell types led to ISC hyperproliferation (Fig. 1E). Therefore, we used the temperature-inducible EC-specific driver *MyoIA-gal4, UAS-gfp; tub-gal80^{ts}* (*MyoIA^{ts}>gfp*) (Jiang et al., 2009) to overexpress either *wg* (*MyoIA^{ts}>wg*) or combined *wg* and *DER^{DN}* (*MyoIA^{ts}>DER^{DN}; wg*) in ECs (Fig. 7H-K). *MyoIA^{ts}>wg* midguts displayed ISC hyperproliferation and upregulation of *upd3* (Fig. 7I,L,M). *MyoIA^{ts}>DER^{DN}; wg* displayed suppression of both Wg-dependent ISC proliferation and *upd3* upregulation (Fig. 7K-M).

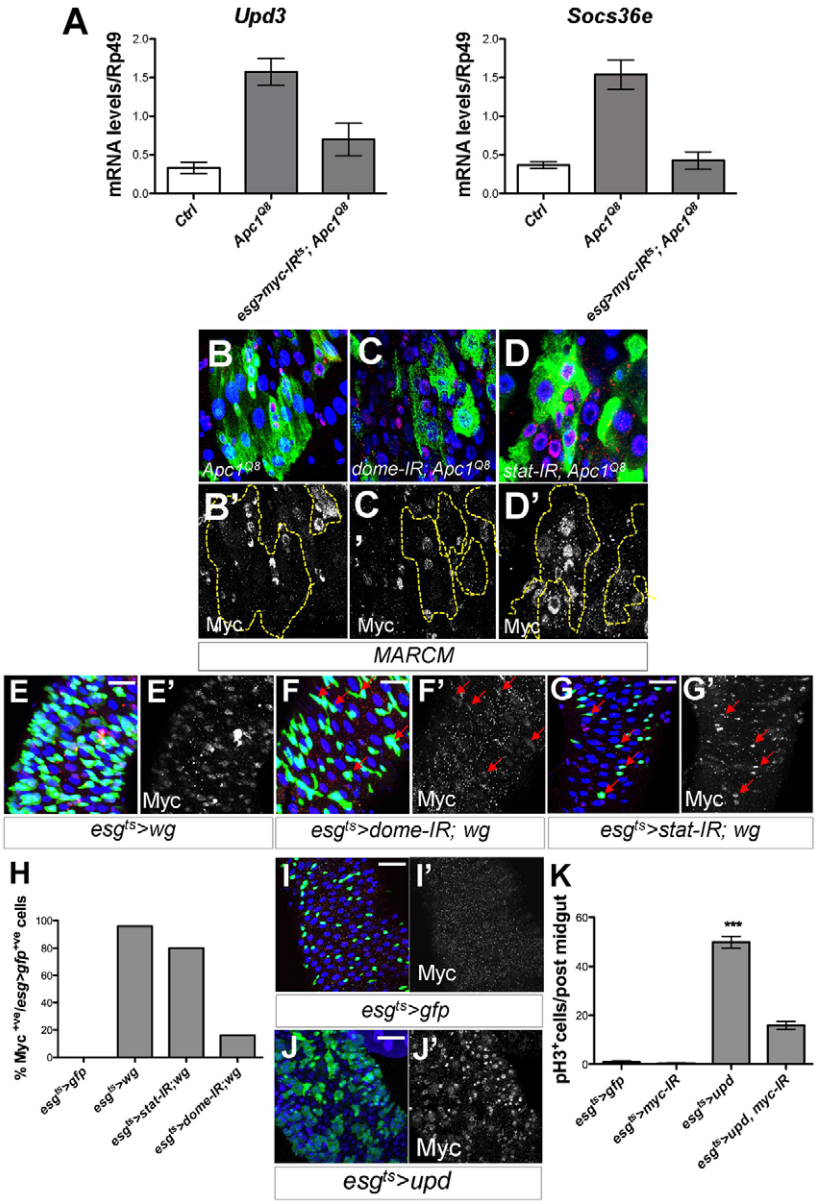

Fig. 6. Jak/Stat signaling activation in *Apc1* midguts requires Myc. (**A**) RT-qPCR for *upd3* and *Socs36e* from 5-day-old control, $Apc1^{Q8}$ and *esg>myc-IR*^{ts}; $Apc1^{Q8}$ whole midguts. Adults were incubated at 29°C from the moment of eclosion. (**B-D'**) 14-day-old MARCM clones (GFP$^+$ or outlined with dashed line) of $Apc1^{Q8}$ (B,B′), *dome-IR;* $Apc1^{Q8}$ (C,C′) or *stat-IR;* $Apc1^{Q8}$ (D,D′) stained with anti-Myc (red or white). (**E-G'**) Immunofluorescence for Myc staining (red or white) in midguts of the indicated genotypes after 14 days of transgene overexpression. (**H**) Quantification of the percentage of Myc$^+$/*esg*$^+$ cells within a preselected region of posterior midguts of the indicated genotypes after 14 days of transgene overexpression. (**I-J'**) Immunofluorescence for Myc staining (red or white) in *esg*^{ts}*>gfp* (I,I′) and *esg*^{ts}*>upd* (J,J′) midguts after 6 days of transgene overexpression. (**K**) Quantification of pH3$^+$ cells in posterior midguts as in I-J′. ***P<0.0001, one-way ANOVA with Bonferroni's multiple comparison test. Error bars indicate s.e.m.

Together, these data suggest that Egfr signaling is a key mediator in the paracrine crosstalk between Wnt/Myc and Jak/Stat signaling in the *Drosophila* midgut.

Conserved Stat3 activation in mouse models and human CRC

Apc loss from mouse ISCs results in rapid adenoma formation (Barker et al., 2009) (Fig. 8A), and widespread deletion from the intestinal epithelium leads to a 'crypt-progenitor cell-like' hyperplastic phenotype (Sansom et al., 2004) (Fig. 8E,F). We used the inducible Cre/Lox system (Sauer, 1998) to knockout *Apc* from the mouse intestine and stained to detect levels of phosphorylated Stat3 (p-Stat3) [Stat3 is the closest homolog of *Drosophila Stat92E* (*marelle*)]. p-Stat3 was normally restricted to the proliferative 'crypt' (Fig. 8A, boxed area C; Fig. 8E; supplementary material Fig. S6A, dashed line), while differentiated villi showed low levels of activated protein (Fig. 8A, boxed area B). We observed ectopic p-Stat3 in intestinal adenomas of *Lgr5-CreER*; $Apc^{fl/fl}$ mice (Barker et al., 2009) (Fig. 8A, arrows and boxed area D; supplementary material Fig. S6B), as well as in the expanded hyperproliferative crypts of *Ah-Cre;* $Apc^{fl/fl}$ (Sansom et al., 2007) intestines (Fig. 8F, dashed line). Suppression of *Apc*-dependent hyperproliferation by c-Myc depletion restored the normal p-Stat3 staining pattern (Fig. 8G, dashed line). Furthermore, immunohistochemical staining of a human CRC tissue microarray for p-Stat3 and c-Myc showed significant positive correlation between protein levels (P<0.0001, Spearman's rank correlation coefficient, n=72; supplementary material Fig. S6C,D). Together, these results point to potential conservation in the role of Jak/Stat signaling in *Apc*-dependent intestinal hyperplasia.

DISCUSSION

Using the *Drosophila* adult midgut as a model system we have uncovered a key set of molecular events that mediate *Apc*-dependent intestinal hyperproliferation. Our results suggest that paracrine crosstalk between Egfr and Jak/Stat signaling is essential for *Apc1*-dependent ISC hyperproliferation in the *Drosophila* midgut (Fig. 9).

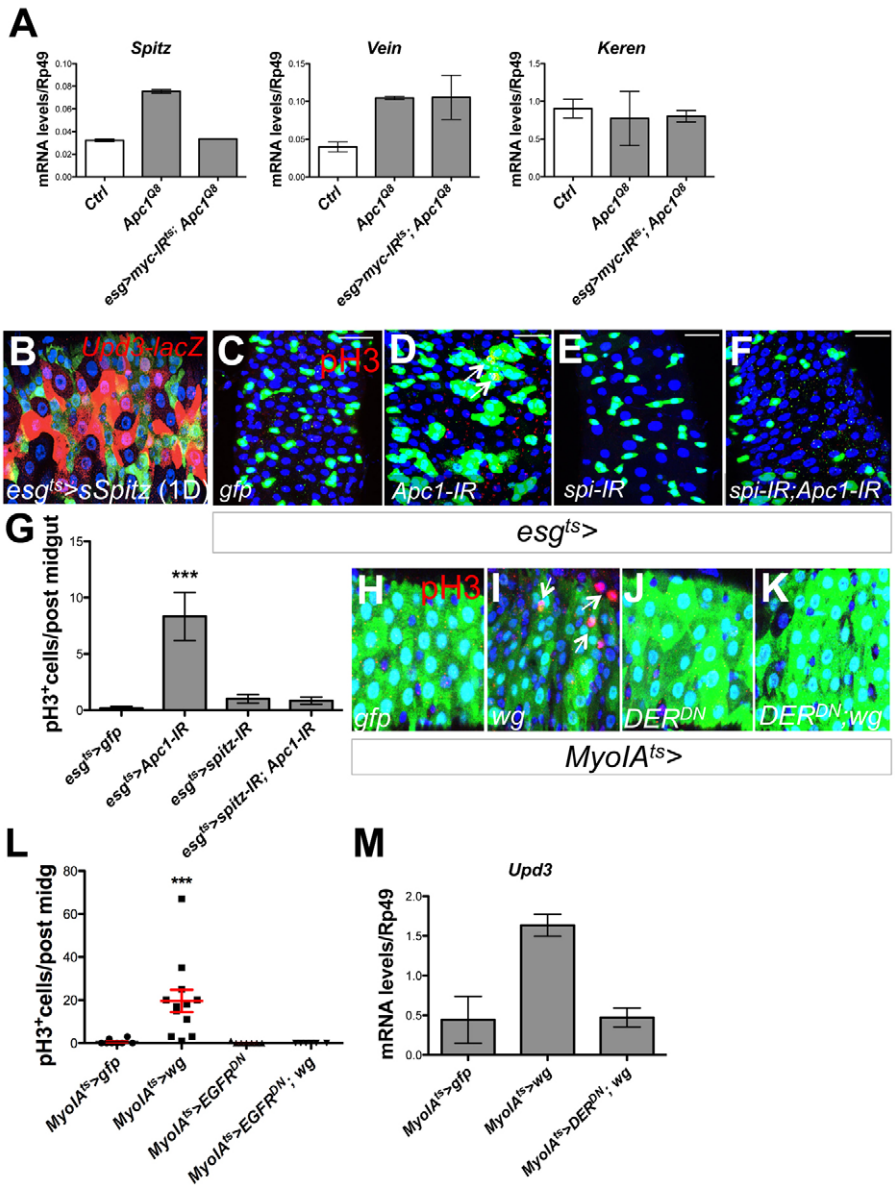

Fig. 7. Egfr signaling mediates Wnt-dependent midgut hyperproliferation. (**A**) RT-qPCR for the EGF ligands *spitz*, *vein* and *Keren* in control, *Apc1*^{Q8} and *esg>myc-IR*^{ts}*; Apc1*^{Q8} whole midguts. (**B**) *upd3-lacZ* expression (red) in response to overexpression of secreted Spitz in progenitor cells (*esg*^{ts}*>sSpitz*; green). *upd3-lacZ* is almost exclusively expressed in large nuclei of *esg*$^{-}$ ECs. (**C-F**) Immunofluorescence of midguts overexpressing *gfp* (C), RNAi for *Apc1* (D; *Apc1-IR*), RNAi for *spitz* (E; *spi-IR*) or combined *spitz* and *Apc1* RNAi (F; *spi-IR; Apc1-IR*) during 14 days in progenitor (*esg*^{ts}) cells (anti-GFP; green). Arrows (D) point to pH3^{+} cells (red). (**G**) Quantification of pH3^{+} cells in posterior midguts as in C-F. ***P<0.0002, one-way ANOVA with Bonferroni's multiple comparison test. (**H-K**) Posterior midguts after 14-day overexpression of *gfp* (H), *wg* (I), *DER*^{DN} (J) or *DER*^{DN}*:wg* (K) in ECs under the control of the *MyoIA*^{ts} driver. Midguts were immunostained for GFP (green) and pH3 (red; arrows). (**L**) Quantification of pH3^{+} cells in posterior midguts as in H-K. ***P<0.0001, one-way ANOVA with Bonferroni's multiple comparison test. (**M**) RT-qPCR for *upd3* in midguts of the indicated genotypes after 14-day transgene overexpression. Error bars indicate s.e.m. Scale bars: 20 μm.

Dependency on Myc and Max

We have previously demonstrated that Myc depletion prevents *Apc*-driven intestinal hyperplasia in the mammalian intestine (Sansom et al., 2007; Athineos and Sansom, 2010). In this study, we provide evidence that such a dependency on Myc is conserved between mammals and *Drosophila*. We further demonstrate that endogenous Myc or Max depletion causes regression of an established *Apc1* phenotype in the intestine. Taken together, these data highlight the importance of developing Myc-targeted therapies to inhibit *Apc1*-deficient cells. Since not all roles of Myc are Max dependent (Steiger et al., 2008), present efforts are focused on developing inhibitors that interfere with Myc binding to Max and would therefore be less toxic. Our data provide the first in vivo evidence in support of the Myc/Max interface as a valid therapeutic target for CRC.

Myc in ISC proliferation and growth

Recent work showed that loss of the tuberous sclerosis complex (TSC) in the *Drosophila* midgut leads to an increase in cell size and inhibition of ISC proliferation (Amcheslavsky et al., 2011). Reduction of endogenous Myc in TSC-deficient midguts restored normal ISC growth and division. These results might appear contradictory to ours, where Myc is a positive regulator of ISC proliferation. However, in both scenarios, modulation of Myc levels restores the normal proliferative rate of ISCs.

Previous work in mouse showed that Myc upregulation is essential for Wnt-driven ISC hyperproliferation in the intestine (Sansom et al., 2007). However, Myc overexpression alone only recapitulates some of the phenotypes of hyperactivated Wnt signaling (Murphy et al., 2008; Finch et al., 2009). Here, we show that overexpression of Myc is capable of mimicking some aspects of high Wnt signaling in the *Drosophila* midgut, such as the activation of Jak/Stat (supplementary material Fig. S7), but is not sufficient to drive ISC hyperproliferation (supplementary material Fig. S7). Multiple lines of evidence have shown that forced overexpression of Myc in *Drosophila* and vertebrate models results in apoptosis partly through activation of p53 (Montero et al., 2008; Murphy et al., 2008; Finch et al., 2009). Therefore, driving ectopic *myc* alone is unlikely to parallel *Apc* deletion in the intestine, where the activation of multiple pathways downstream of Wnt signaling is likely to contribute cooperatively to hyperproliferation.

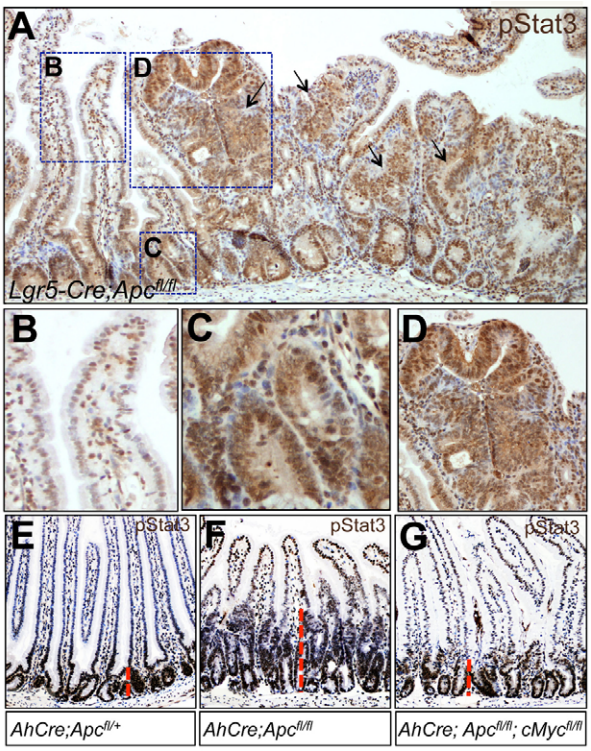

Fig. 8. Conserved Stat3 activation in mouse and human colorectal tumor samples. (**A-D**) Small intestine from *Lgr5-Cre; Apc*$^{fl/fl}$ mice immunostained for p-Stat3 to detect the activated form of the protein. (B-D) Magnified views of the boxed areas in A, showing differentiated villi (B), proliferative crypts (C) and hyperplastic adenomas (D). Arrows in A point to adenomas, which showed ectopic p-Stat3 staining. (**E-G**) Small intestines from *AhCre; Apc*$^{fl/+}$ (E), *AhCre; Apc*$^{fl/fl}$ (F) and *AhCre; Apc*$^{fl/fl}$*; c-Myc*$^{fl/fl}$ (G) mice immunostained for p-Stat3. Dashed lines delimit the proliferative domain. Expansion of the proliferative zone in response to *Apc* loss directly correlated with the levels of p-Stat3 (compare F with E). Consequently, intestines from *Apc*$^{fl/fl}$*; c-Myc*$^{fl/fl}$ mice showed a restored p-Stat3 staining domain (compare G with E,F).

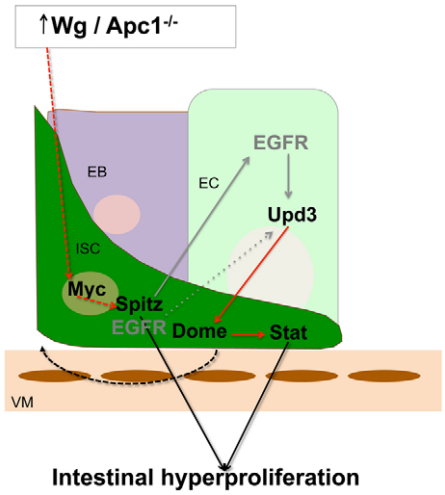

Fig. 9. Paracrine Egfr and Jak/Stat signaling crosstalk mediates *Apc1*-dependent intestinal hyperproliferation. Loss of *Apc1* in the midgut leads to the production of Spitz and Upd3 in ISCs and ECs, respectively. Upregulation of both ligands requires previous activation of Myc in ISCs. Activated Jak/Stat signaling in turn contributes to Myc upregulation in a Dome-dependent manner. Apc1/Myc-dependent activation of Egfr and Jak/Stat signaling leads to intestinal hyperproliferation. Alternative possibilities for Upd3 upregulation by Spitz/Egfr signaling are shown in gray. EB, enteroblast; EC, enterocyte; ISC, intestinal stem cell; VM, visceral muscle.

Jak/Stat signaling activation in *Apc*-driven intestinal hyperplasia

Understanding the contribution of Jak/Stat signaling to the *Apc* phenotype in the mammalian intestine has been complicated by genetic redundancy between Stat transcription factors. Constitutive deletion of *Stat3* within the intestinal epithelium slowed tumor formation in the *Apc*$^{Min/+}$ mouse, but the tumors that arose were more aggressive and ectopically expressed Stat1 (Musteanu et al., 2010). Using the *Drosophila* midgut we provide direct in vivo evidence that activation of Jak/Stat signaling downstream of Apc1/Myc mediates *Apc1*-dependent hyperproliferation.

Our data on the *Drosophila* midgut and in mouse and human tissue samples suggest that blocking Jak/Stat activation could represent an efficacious therapeutic strategy to treat CRC. Currently, there are a number of Jak2 inhibitors under development (Che et al., 2009; Quintás-Cardama et al., 2010) and it would be of great interest to examine whether any of these could modify the phenotypes associated with *Apc* loss.

Non-autonomous production of Upd and the role of Egfr signaling

Previous studies have demonstrated that ECs are the main source of Upds/interleukins in the midgut epithelium (Jiang et al., 2009). Our results show that activation of Wnt/Myc signaling in ISCs leads to non-autonomous upregulation of *upd3* within ECs. Furthermore, Spitz/Egfr signaling appears to mediate the paracrine crosstalk between Wnt/Myc and Jak/Stat in the midgut. Overexpression of a dominant-negative Egfr in ECs blocks *upd3* upregulation and ISC hyperproliferation in response to high Wnt signaling (Fig. 7). A previous EC-specific role for Egfr has been demonstrated during midgut remodeling upon bacterial damage (Buchon et al., 2010). Nevertheless, the downstream signaling that mediates such a role of Egfr remains unclear given that the activation of downstream MAPK/ERK occurs exclusively within ISCs (Buchon et al., 2010; Biteau and Jasper, 2011; Jiang et al., 2011) (data not shown). Therefore, the current evidence would suggest that Egfr activity in ECs does not involve cell-autonomous ERK activation. Consistent with these observations, we did not detect p-ERK (Rolled – FlyBase) localization outside ISCs in response to either *Apc* loss or overexpression of *wg* in the *Drosophila* midgut (data not shown). Reports on the *Apc* murine intestine have also failed to detect robust ERK activation (Sansom et al., 2006; Haigis et al., 2008). Since MAPK/ERK is only one of the pathways activated downstream of Egfr, it is possible that ERK-independent mechanisms are involved. It is important to explore this further because ERK-independent roles of Egfr signaling have not yet been reported in *Drosophila*. Thus, what mediates Upd3 upregulation in ECs in response to Egfr signaling activation and whether Spitz-dependent upregulation of Upd3 involves a direct role of Egfr in ECs remain unclear. A potential alternative explanation is that intermediate factors induced in response to Spitz/Egfr activation in ISCs might drive Upd3 expression (Fig. 9).

In summary, we have elucidated a novel molecular signaling network leading to Wnt-dependent intestinal hyperproliferation. Given the preponderance of *APC* mutations in CRC, the integration of Egfr and Jak/Stat activation might be a conserved initiating event in the disease.

Acknowledgements
We thank Yashi Ahmed, Peter Gallant, Matthew Freeman, Gines Morata, Bruce Edgar, Nicolas Buchon, Shigeo Hayashi, William Chia, Huaqui Jiang, David Bilder, DGRC, VDRC, Bloomington Stock Center and the Developmental Studies Hybridoma Bank for generously providing fly lines and reagents; Colin Nixon for immunohistochemistry and H+E staining of fly midguts; Alessandro Scopelliti for providing the Fig. S5D,D′ image; and Karen Strathdee for technical assistance.

Funding
M.V. and O.J.S. are Cancer Research UK investigators. This work was partly funded by a National Centre for the Replacement, Refinement and Reduction of Animals (NC3Rs) grant; J.B.C. is funded by Marie Curie and European Molecular Biology Organization (EMBO) fellowships.

Competing interests statement
The authors declare no competing financial interests.

Supplementary material
Supplementary material available online at
http://dev.biologists.org/lookup/suppl/doi:10.1242/dev.078261/-/DC1

References

Ahmed, Y., Hayashi, S., Levine, A. and Wieschaus, E. (1998). Regulation of armadillo by a Drosophila APC inhibits neuronal apoptosis during retinal development. *Cell* **93**, 1171-1182.
Ahmed, Y., Nouri, A. and Wieschaus, E. (2002). Drosophila Apc1 and Apc2 regulate wingless transduction throughout development. *Development* **129**, 1751-1762.
Amcheslavsky, A., Ito, N., Jiang, J. and Ip, Y. T. (2011). Tuberous sclerosis complex and Myc coordinate the growth and division of Drosophila intestinal stem cells. *J. Cell Biol.* **193**, 695-710.
Andreu, P., Colnot, S., Godard, C., Gad, S., Chafey, P., Niwa-Kawakita, M., Laurent-Puig, P., Kahn, A., Robine, S., Perret, C. et al. (2005). Crypt-restricted proliferation and commitment to the Paneth cell lineage following Apc loss in the mouse intestine. *Development* **132**, 1443-1451.
Athineos, D. and Sansom, O. J. (2010). Myc heterozygosity attenuates the phenotypes of APC deficiency in the small intestine. *Oncogene* **29**, 2585-2590.
Bach, E. A., Ekas, L. A., Ayala-Camargo, A., Flaherty, M. S., Lee, H., Perrimon, N. and Baeg, G.-H. (2007). GFP reporters detect the activation of the Drosophila JAK/STAT pathway in vivo. *Gene Expr. Patterns* **7**, 323-331.
Barker, N., van Es, J. H., Kuipers, J., Kujala, P., van den Born, M., Cozijnsen, M., Haegebarth, A., Korving, J., Begthel, H., Peters, P. J. and Clevers, H. (2007). Identification of stem cells in small intestine and colon by marker gene Lgr5. *Nature* **449**, 1003-1007.
Barker, N., Ridgway, R. A., van Es, J. H., van de Wetering, M., Begthel, H., van den Born, M., Danenberg, E., Clarke, A. R., Sansom, O. J. and Clevers, H. (2009). Crypt stem cells as the cells-of-origin of intestinal cancer. *Nature* **457**, 608-611.
Beebe, K., Lee, W. C. and Micchelli, C. A. (2010). JAK/STAT signaling coordinates stem cell proliferation and multilineage differentiation in the Drosophila intestinal stem cell lineage. *Dev. Biol.* **338**, 28-37.
Biteau, B. and Jasper, H. (2011). EGF signaling regulates the proliferation of intestinal stem cells in Drosophila. *Development* **138**, 1045-1055.
Buchon, N., Broderick, N. A., Chakrabarti, S. and Lemaitre, B. (2009). Invasive and indigenous microbiota impact intestinal stem cell activity through multiple pathways in Drosophila. *Genes Dev.* **23**, 2333-2344.
Buchon, N., Broderick, N. A., Kuraishi, T. and Lemaitre, B. (2010). Drosophila EGFR pathway coordinates stem cell proliferation and gut remodeling following infection. *BMC Biol.* **8**, 152.
Casali, A. and Batlle, E. (2009). Intestinal stem cells in mammals and Drosophila. *Cell Stem Cell* **4**, 124-127.
Che, Y., Hou, S., Kang, Z. and Lin, Q. (2009). Serenoa repens induces growth arrest and apoptosis of human multiple myeloma cells via inactivation of STAT 3 signaling. *Oncol. Rep.* **22**, 377-383.
Cordero, J., Vidal, M. and Sansom, O. (2009). APC as a master regulator of intestinal homeostasis and transformation: from flies to vertebrates. *Cell Cycle* **8**, 2927-2932.
Cordero, J. B., Stefanatos, R. K., Scopelliti, A., Vidal, M. and Sansom, O. J. (2012). Inducible progenitor-derived wingless regulates adult midgut regeneration in Drosophila. *EMBO J.* **31**, 3901-3917.
Felsher, D. W. (2008). Tumor dormancy and oncogene addiction. *APMIS* **116**, 629-637.
Felsher, D. W. and Bishop, J. M. (1999). Reversible tumorigenesis by MYC in hematopoietic lineages. *Mol. Cell* **4**, 199-207.
Finch, A. J., Soucek, L., Junttila, M. R., Swigart, L. B. and Evan, G. I. (2009). Acute overexpression of Myc in intestinal epithelium recapitulates some but not all the changes elicited by Wnt/beta-catenin pathway activation. *Mol. Cell. Biol.* **29**, 5306-5315.
Haigis, K. M., Kendall, K. R., Wang, Y., Cheung, A., Haigis, M. C., Glickman, J. N., Niwa-Kawakita, M., Sweet-Cordero, A., Sebolt-Leopold, J., Shannon, K. M. et al. (2008). Differential effects of oncogenic K-Ras and N-Ras on proliferation, differentiation and tumor progression in the colon. *Nat. Genet.* **40**, 600-608.
Holstege, F. C. and Clevers, H. (2006). Transcription factor target practice. *Cell* **124**, 21-23.
Ireland, H., Kemp, R., Houghton, C., Howard, L., Clarke, A. R., Sansom, O. J. and Winton, D. J. (2004). Inducible Cre-mediated control of gene expression in the murine gastrointestinal tract: effect of loss of beta-catenin. *Gastroenterology* **126**, 1236-1246.
Jiang, H., Patel, P. H., Kohlmaier, A., Grenley, M. O., McEwen, D. G. and Edgar, B. A. (2009). Cytokine/Jak/Stat signaling mediates regeneration and homeostasis in the Drosophila midgut. *Cell* **137**, 1343-1355.
Jiang, H., Grenley, M. O., Bravo, M. J., Blumhagen, R. Z. and Edgar, B. A. (2011). EGFR/Ras/MAPK signaling mediates adult midgut epithelial homeostasis and regeneration in Drosophila. *Cell Stem Cell* **8**, 84-95.
Johnston, L. A., Prober, D. A., Edgar, B. A., Eisenman, R. N. and Gallant, P. (1999). Drosophila myc regulates cellular growth during development. *Cell* **98**, 779-790.
Karpowicz, P., Perez, J. and Perrimon, N. (2010). The Hippo tumor suppressor pathway regulates intestinal stem cell regeneration. *Development* **137**, 4135-4145.
Kinzler, K. W., Nilbert, M. C., Su, L. K., Vogelstein, B., Bryan, T. M., Levy, D. B., Smith, K. J., Preisinger, A. C., Hedge, P., McKechnie, D. et al. (1991). Identification of FAP locus genes from chromosome 5q21. *Science* **253**, 661-665.
Korinek, V., Barker, N., Morin, P. J., van Wichen, D., de Weger, R., Kinzler, K. W., Vogelstein, B. and Clevers, H. (1997). Constitutive transcriptional activation by a beta-catenin-Tcf complex in APC-/- colon carcinoma. *Science* **275**, 1784-1787.
Korinek, V., Barker, N., Moerer, P., van Donselaar, E., Huls, G., Peters, P. J. and Clevers, H. (1998). Depletion of epithelial stem-cell compartments in the small intestine of mice lacking Tcf-4. *Nat. Genet.* **19**, 379-383.
Lee, T. and Luo, L. (2001). Mosaic analysis with a repressible cell marker (MARCM) for Drosophila neural development. *Trends Neurosci.* **24**, 251-254.
Lee, W.-C., Beebe, K., Sudmeier, L. and Micchelli, C. A. (2009). Adenomatous polyposis coli regulates Drosophila intestinal stem cell proliferation. *Development* **136**, 2255-2264.
Lin, G., Xu, N. and Xi, R. (2008). Paracrine wingless signalling controls self-renewal of Drosophila intestinal stem cells. *Nature* **455**, 1119-1123.
Lin, G., Xu, N. and Xi, R. (2010). Paracrine unpaired signaling through the JAK/STAT pathway controls self-renewal and lineage differentiation of Drosophila intestinal stem cells. *J. Mol. Cell Biol.* **2**, 37-49.
Micchelli, C. A. and Perrimon, N. (2006). Evidence that stem cells reside in the adult Drosophila midgut epithelium. *Nature* **439**, 475-479.
Montero, L., Müller, N. and Gallant, P. (2008). Induction of apoptosis by Drosophila Myc. *Genesis* **46**, 104-111.
Murphy, D. J., Junttila, M. R., Pouyet, L., Karnezis, A., Shchors, K., Bui, D. A., Brown-Swigart, L., Johnson, L. and Evan, G. I. (2008). Distinct thresholds govern Myc's biological output in vivo. *Cancer Cell* **14**, 447-457.
Musteanu, M., Blaas, L., Mair, M., Schlederer, M., Bilban, M., Tauber, S., Esterbauer, H., Mueller, M., Casanova, E., Kenner, L. et al. (2010). Stat3 is a negative regulator of intestinal tumor progression in Apc(Min) mice. *Gastroenterology* **138**, 1003-1011.
Ohlstein, B. and Spradling, A. (2006). The adult Drosophila posterior midgut is maintained by pluripotent stem cells. *Nature* **439**, 470-474.
Ohlstein, B. and Spradling, A. (2007). Multipotent Drosophila intestinal stem cells specify daughter cell fates by differential notch signaling. *Science* **315**, 988-992.
Quintás-Cardama, A., Vaddi, K., Liu, P., Manshouri, T., Li, J., Scherle, P. A., Caulder, E., Wen, X., Li, Y., Waeltz, P. et al. (2010). Preclinical characterization of the selective JAK1/2 inhibitor INCB018424: therapeutic implications for the treatment of myeloproliferative neoplasms. *Blood* **115**, 3109-3117.
Reed, K. R., Athineos, D., Meniel, V. S., Wilkins, J. A., Ridgway, R. A., Burke, Z. D., Muncan, V., Clarke, A. R. and Sansom, O. J. (2008). B-catenin deficiency, but not Myc deletion, suppresses the immediate phenotypes of APC loss in the liver. *Proc. Natl. Acad. Sci. USA* **105**, 18919-18923.
Ren, F., Wang, B., Yue, T., Yun, E.-Y., Ip, Y. T. and Jiang, J. (2010). Hippo signaling regulates Drosophila intestine stem cell proliferation through multiple pathways. *Proc. Natl. Acad. Sci. USA* **107**, 21064-21069.
Sansom, O. J., Reed, K. R., Hayes, A. J., Ireland, H., Brinkmann, H., Newton, I. P., Batlle, E., Simon-Assmann, P., Clevers, H., Nathke, I. S. et al. (2004). Loss of Apc in vivo immediately perturbs Wnt signaling, differentiation, and migration. *Genes Dev.* **18**, 1385-1390.
Sansom, O. J., Meniel, V., Wilkins, J. A., Cole, A. M., Oien, K. A., Marsh, V., Jamieson, T. J., Guerra, C., Ashton, G. H., Barbacid, M. et al. (2006). Loss of Apc allows phenotypic manifestation of the transforming properties of an

endogenous K-ras oncogene in vivo. *Proc. Natl. Acad. Sci. USA* **103**, 14122-14127.
Sansom, O. J., Meniel, V. S., Muncan, V., Phesse, T. J., Wilkins, J. A., Reed, K. R., Vass, J. K., Athineos, D., Clevers, H. and Clarke, A. R. (2007). Myc deletion rescues Apc deficiency in the small intestine. *Nature* **446**, 676-679.
Sauer, B. (1998). Inducible gene targeting in mice using the Cre/lox system. *Methods* **14**, 381-392.
Shaw, R. L., Kohlmaier, A., Polesello, C., Veelken, C., Edgar, B. A. and Tapon, N. (2010). The Hippo pathway regulates intestinal stem cell proliferation during Drosophila adult midgut regeneration. *Development* **137**, 4147-4158.
Smith-Bolton, R. K., Worley, M. I., Kanda, H. and Hariharan, I. K. (2009). Regenerative growth in Drosophila imaginal discs is regulated by Wingless and Myc. *Dev. Cell* **16**, 797-809.
Soucek, L., Whitfield, J., Martins, C. P., Finch, A. J., Murphy, D. J., Sodir, N. M., Karnezis, A. N., Swigart, L. B., Nasi, S. and Evan, G. I. (2008). Modelling Myc inhibition as a cancer therapy. *Nature* **455**, 679-683.
Steiger, D., Furrer, M., Schwinkendorf, D. and Gallant, P. (2008). Max-independent functions of Myc in Drosophila melanogaster. *Nat. Genet.* **40**, 1084-1091.
Trumpp, A., Refaeli, Y., Oskarsson, T., Gasser, S., Murphy, M., Martin, G. R. and Bishop, J. M. (2001). c-Myc regulates mammalian body size by controlling cell number but not cell size. *Nature* **414**, 768-773.
van de Wetering, M., Sancho, E., Verweij, C., de Lau, W., Oving, I., Hurlstone, A., van der Horn, K., Batlle, E., Coudreuse, D., Haramis, A. P. et al. (2002). The beta-catenin/TCF-4 complex imposes a crypt progenitor phenotype on colorectal cancer cells. *Cell* **111**, 241-250.
Van der Flier, L. G., Sabates-Bellver, J., Oving, I., Haegebarth, A., De Palo, M., Anti, M., Van Gijn, M. E., Suijkerbuijk, S., Van de Wetering, M., Marra, G. et al. (2007). The Intestinal Wnt/TCF Signature. *Gastroenterology* **132**, 628-632.
Vincent, J. P., Kolahgar, G., Gagliardi, M. and Piddini, E. (2011). Steep differences in wingless signaling trigger Myc-independent competitive cell interactions. *Dev. Cell* **21**, 366-374.
Vita, M. and Henriksson, M. (2006). The Myc oncoprotein as a therapeutic target for human cancer. *Semin. Cancer Biol.* **16**, 318-330.
Yamashita, Y. M., Jones, D. L. and Fuller, M. T. (2003). Orientation of asymmetric stem cell division by the APC tumor suppressor and centrosome. *Science* **301**, 1547-1550.

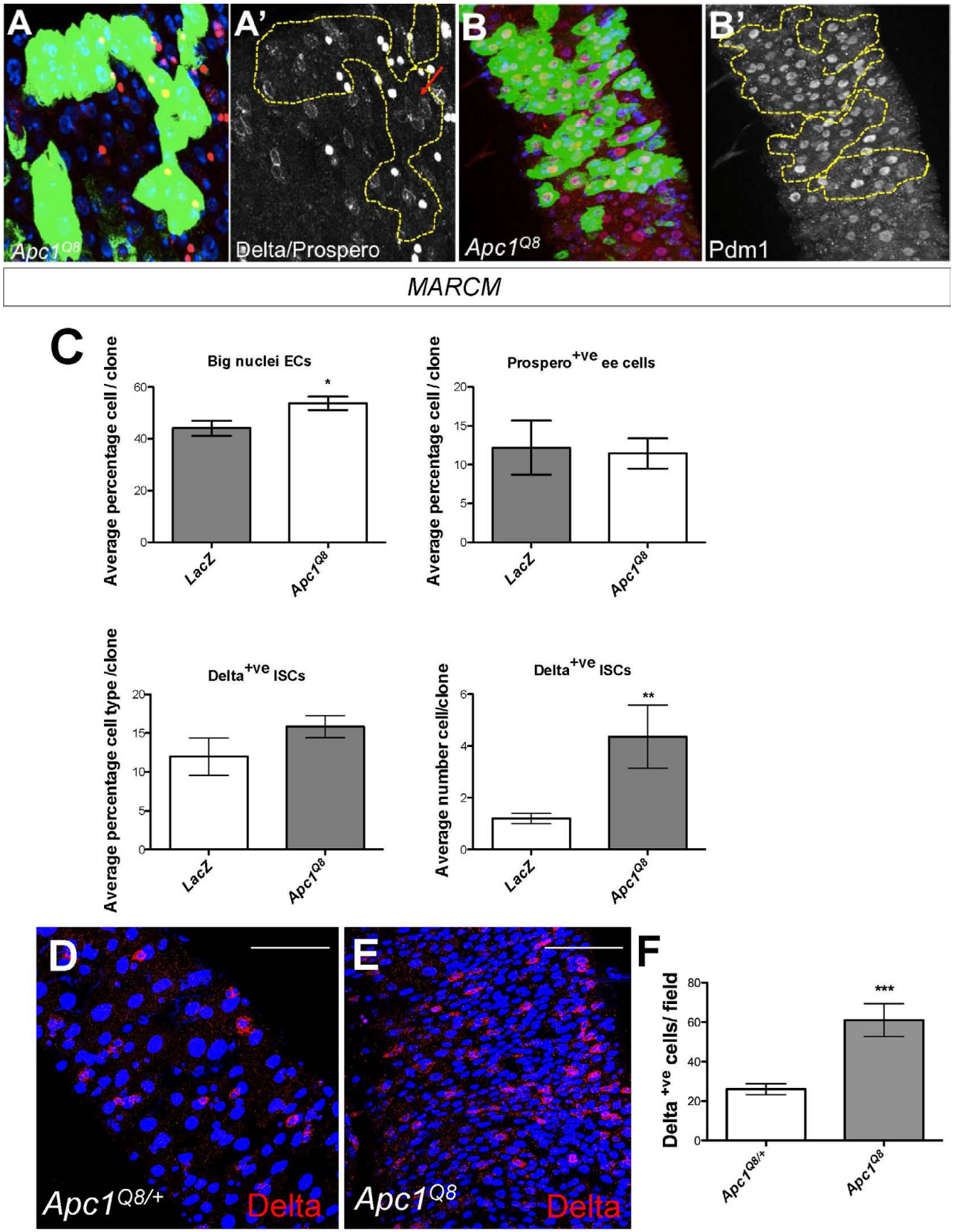

Fig. S1. Loss of *Apc1* does not affect ISC differentiation in the adult *Drosophila* midgut. (**A-B′**) 14-day-old $Apc1^{-/-}$ ($Apc1^{Q8}$) MARCM clones (GFP$^+$ or outlined by dashed line). Clones were immunostained for Delta and Prospero (A,A′, red or white) to label ISCs and enteroendocrine (ee) cells, respectively, or for Pdm1 (B,B′, red or white) to label enterocytes (ECs). (**C**) The average percentage of large nuclei ECs (*P=0.02, Student's t-test), Prospero$^+$ and Delta$^+$ cells and the average number of Delta$^+$ cells (lower right panel; **P=0.01, Student's t-test) in control (*lacZ*) and $Apc1^{Q8}$ MARCM clones. (**D**,**E**) Whole $Apc1^{Q8/+}$ (D) and $Apc1^{Q8}$ (E) midguts stained with anti-Delta (red). (**F**) Quantification of the total number of Delta$^+$ cells (***P<0.007, Student's t-test) within a pre-established field of $Apc1^{Q8/+}$ and $Apc1^{Q8}$ posterior midguts. DAPI (blue) was used to label nuclei. Scale bars: 40 μm.

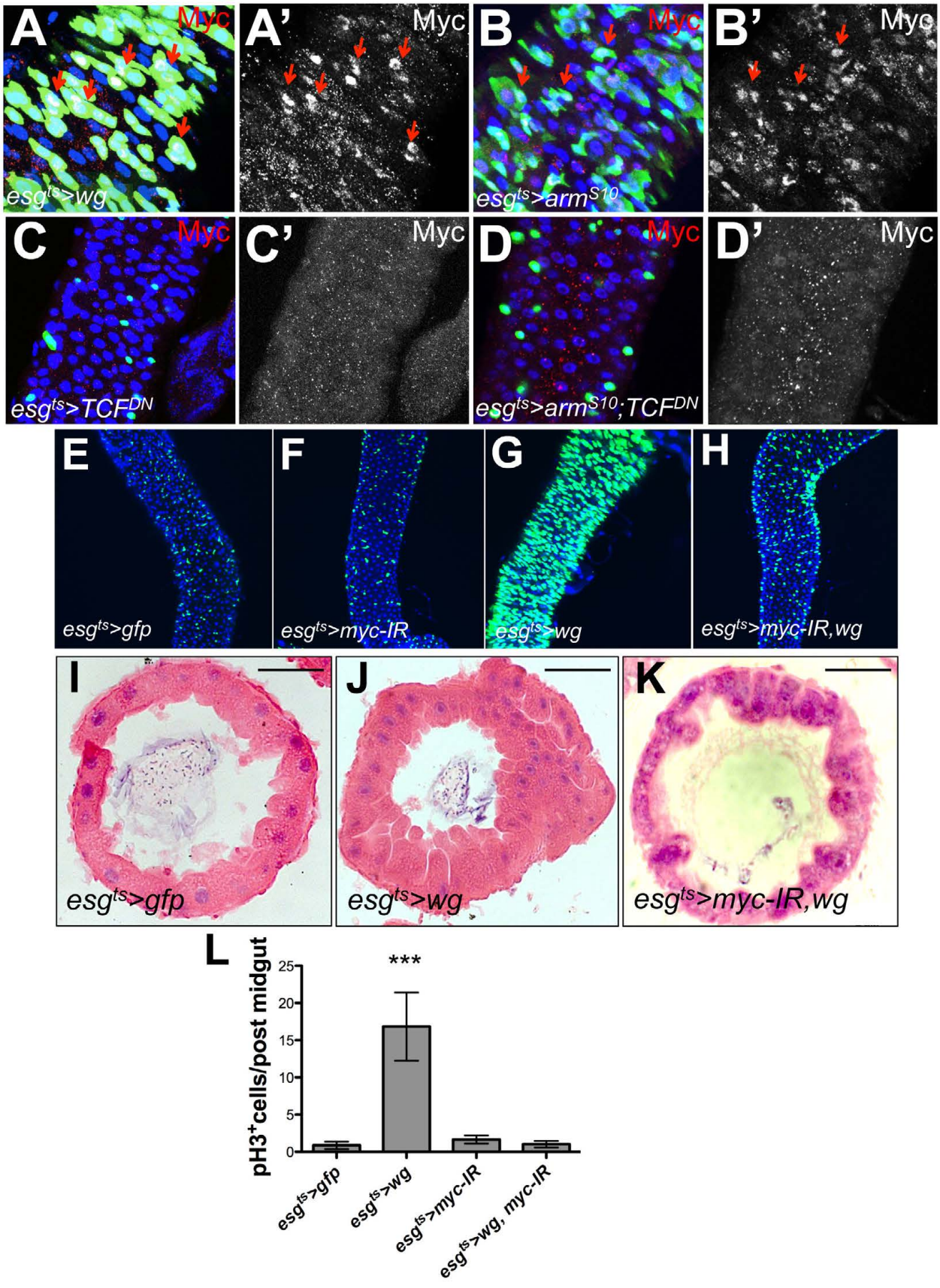

Fig. S2. Myc upregulation mediates Wnt-dependent hyperproliferation in the *Drosophila* midgut. (**A-D′**) Posterior midguts of the indicated genotypes after 14 days of transgene overexpression and stained with anti-GFP (green) to label *esg*$^+$ cells and anti-Myc (red or white). (**E-H**) Immunofluorescence of midguts of the indicated genotypes after 14 days of transgene overexpression and stained with anti-GFP (green) to label *esg*$^+$ cells. DAPI (blue) labels nuclei. (**I-K**) Immunohistochemistry and H+E staining of midguts as in E,G,H. (**L**) Quantification of pH3$^+$ cells in midguts of the indicated genotypes after 14 days of transgene expression. ***P<0.0001, one-way ANOVA with Bonferroni's multiple comparison test. Scale bars: 40 μm.

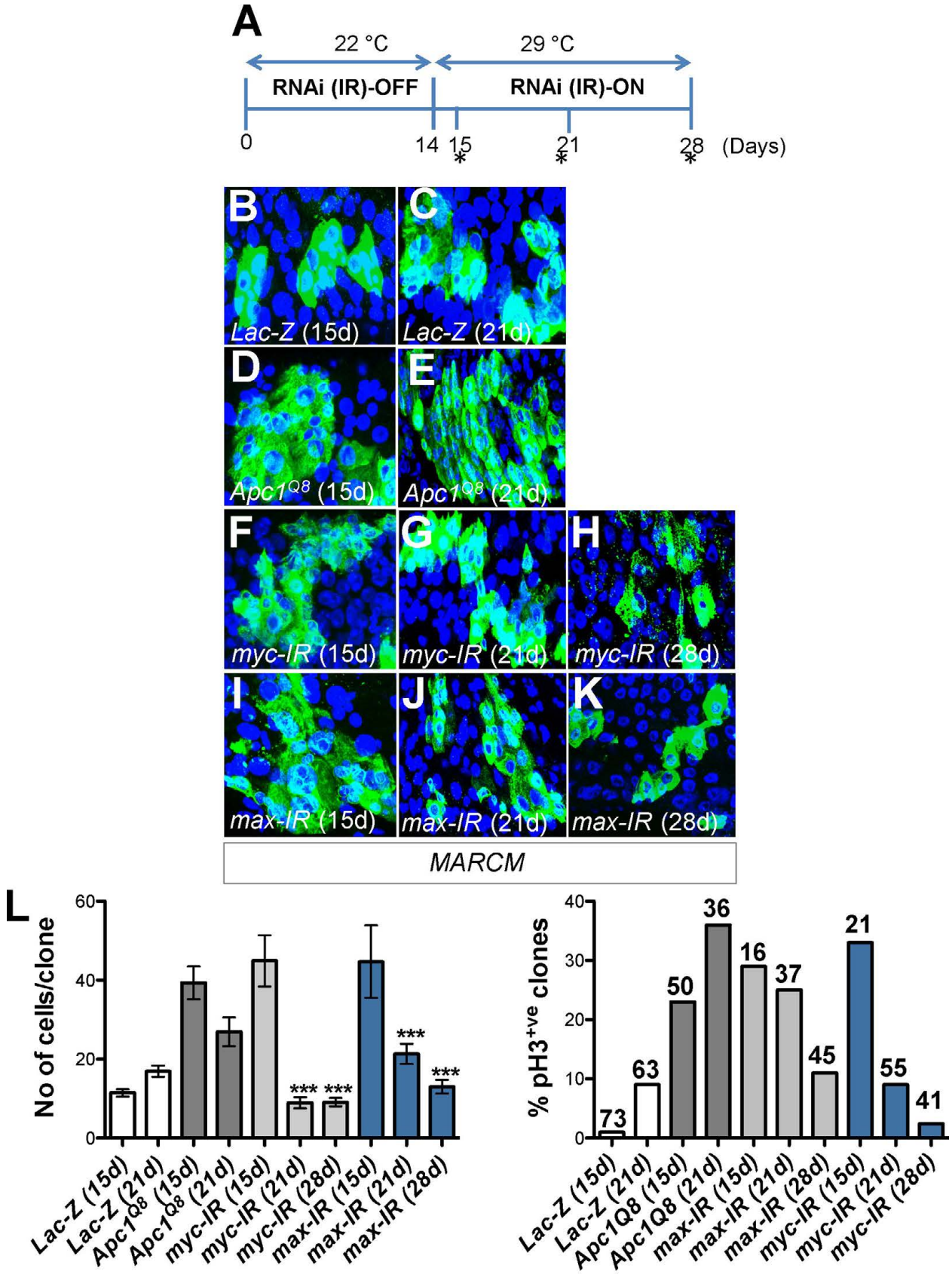

Fig. S3. Myc and Max depletion regresses pre-established intestinal hyperproliferation by *Apc1* loss. (**A**) Experimental setup. Flies were maintained at 22°C for the first 14 days after clonal induction (ACI). This was followed by incubation at 29°C for 1, 7 or 14 days. Cohorts were analyzed at the time points indicated by asterisks. (**B-K**) Control (*lacZ*) (B,C) and $Apc1^{Q8}$ MARCM clones (D,E) were analyzed 15 and 21 days ACI and compared with 14-day-old $Apc1^{Q8}$ MARCM clones in which temperature-sensitive RNAi transgenes for *myc* or *Max* (*myc-IR* and *max-IR*, respectively) were induced for an additional 1 (F,I; 15d), 7 (G,J; 21d) or 14 days (H,K; 28d) at 29°C. Clones are labeled with GFP (green) and DAPI (blue) labels nuclei. (**L**) Quantification of the number of cells per clone (left) and percentage of clones with $pH3^+$ cells (right) for the different conditions described in B-K. Note that knockdown of *myc* or *Max* regressed the size of $Apc1^{Q8}$ clones (L). ***$P<0.0001$, one-way ANOVA with Bonferroni's multiple comparison test. Numbers inside bars indicate the total number of clones scored.

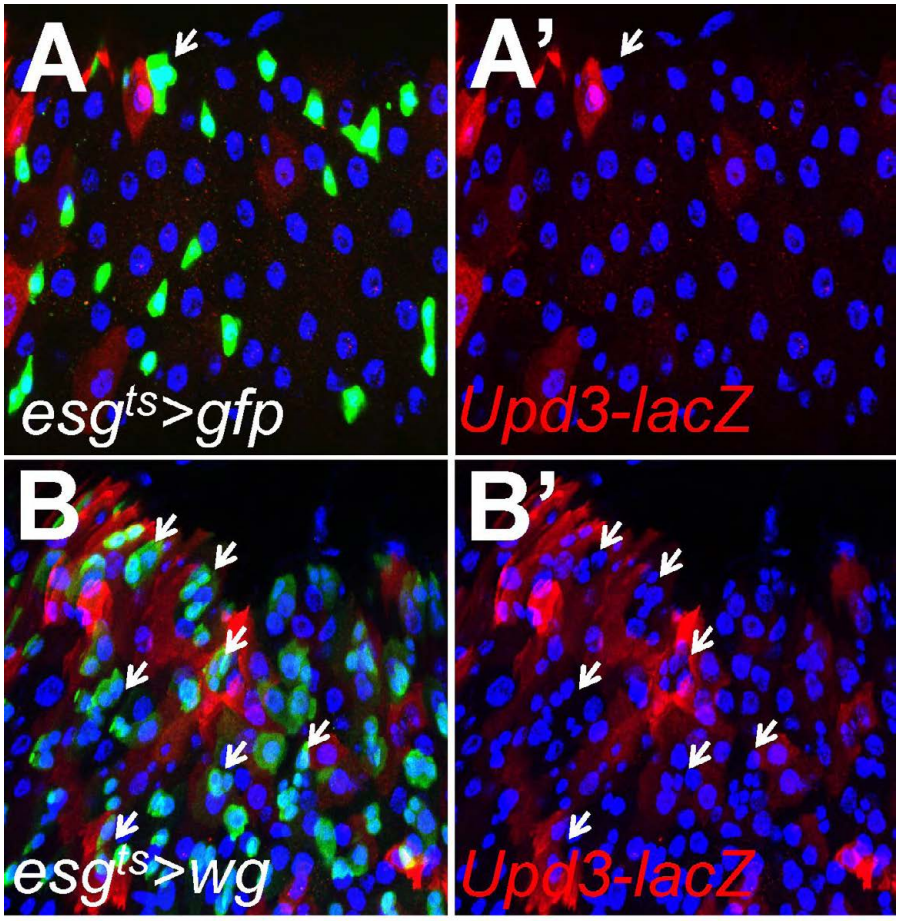

Fig. S4. Overexpression of Wg in ISCs leads to Upd3 upregulation in ECs. *upd3-lacZ* reporter expression (red) in posterior midguts following 14 days of *esg*^{ts}*>gfp* (**A**,**A′**) or *esg*^{ts}*>wg* (**B**,**B′**) expression. Arrows point to ISCs/EBs labeled with *esg>gfp* (green). Overexpression of Wg in ISCs resulted in non-autonomous activation of *upd3* in ECs.

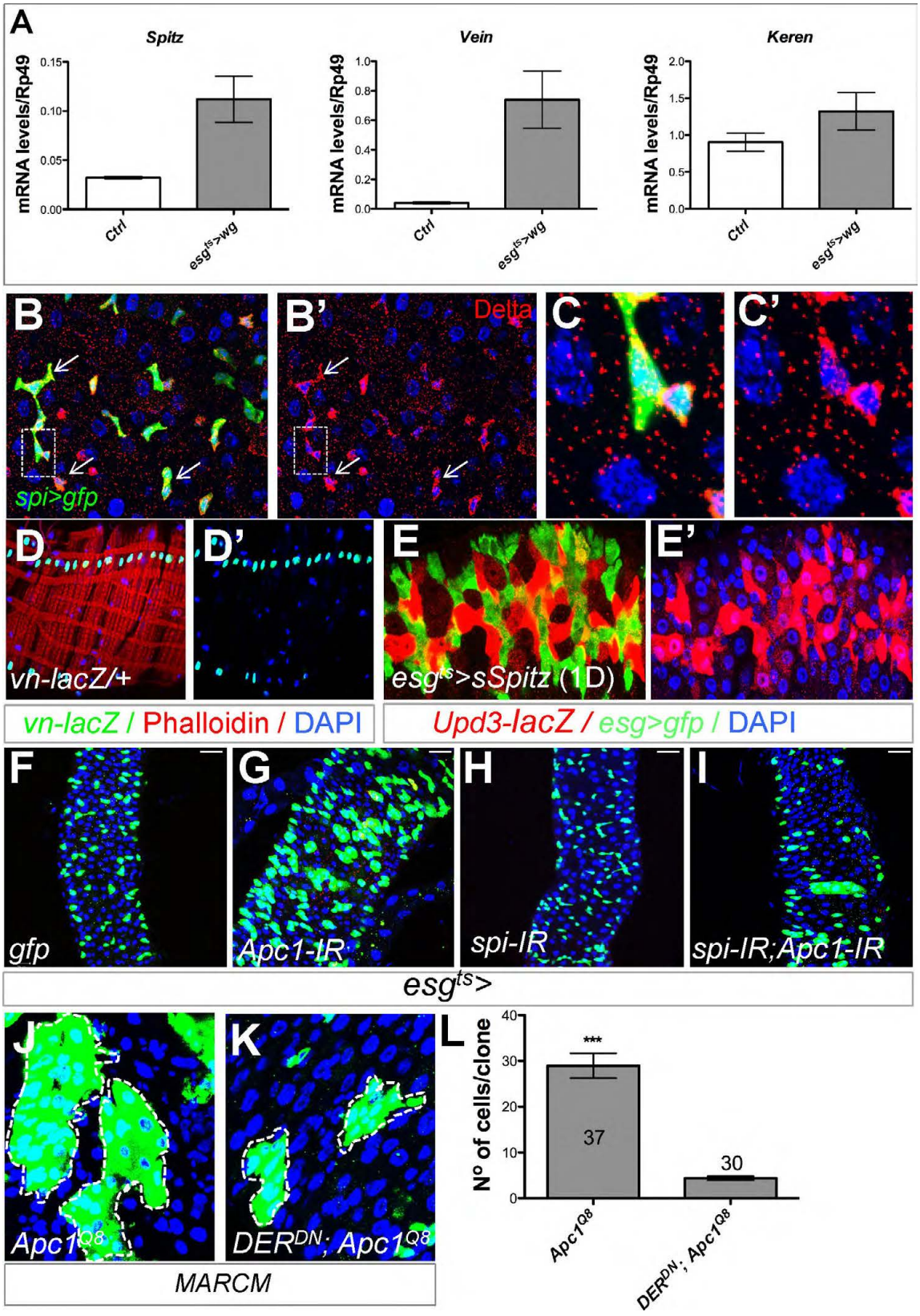

Fig. S5. Spitz/Egfr signaling mediates *Apc1*-dependent midgut hyperproliferation. (**A**) RT-qPCR of the EGF ligands *spitz*, *vein* and *Keren* in control (Ctrl) and *esg*^{ts}*>wg* midguts after 14 days of transgene expression. (**B-C′**) Midguts expressing *gfp* under the control of the *spitz-gal4* reporter (*spi>gfp*) were stained with anti-GFP (B,C, green) and anti-Delta (B-C′, red). (C,C′) Magnified views of the boxed areas in B,B′. Arrows point to *spi>gfp*/Delta^{+} ISCs. *spitz* was expressed in Delta^{+} ISCs and enteroblasts (Delta^{-}) (C,C′). (**D**,**D′**) *vein* expression in the visceral muscle (phalloidin, red) as monitored by a *vein-lacZ* reporter line (green). (**E**,**E′**) *upd3-lacZ* expression (red) in response to overexpression of secreted Spitz in progenitor cells (*esg*^{ts}*>sSpitz*, green). *upd3-lacZ* is almost exclusively expressed in large nuclei, *esg*$^{-}$ ECs. DAPI (blue) labels nuclei. (**F-I**) Immunofluorescence of midguts overexpressing *gfp* (F), RNAi for *Apc1* (G; *Apc1-IR*), RNAi for *Spitz* (H; *spi-IR*) or combined *spitz* and *Apc1* RNAi (I; *spi-IR; Apc1-IR*) during 14 days in progenitor (*esg*^{ts}) cells (anti-GFP, green). (**J**,**K**) 14-day-old *Apc1*^{Q8} MARCM clones (J) and clones with combined expression a dominant-negative form of the EGF receptor (*DER*^{DN}*; Apc1*^{Q8}) (K); clones are labeled with GFP and outlined by dashed line. (**L**) Quantification of the number of cells per clone from J,K. ***P<0.0001, Student's t-test. Numbers in bars indicate the total number of clones scored. Scale bars: 20 μm.

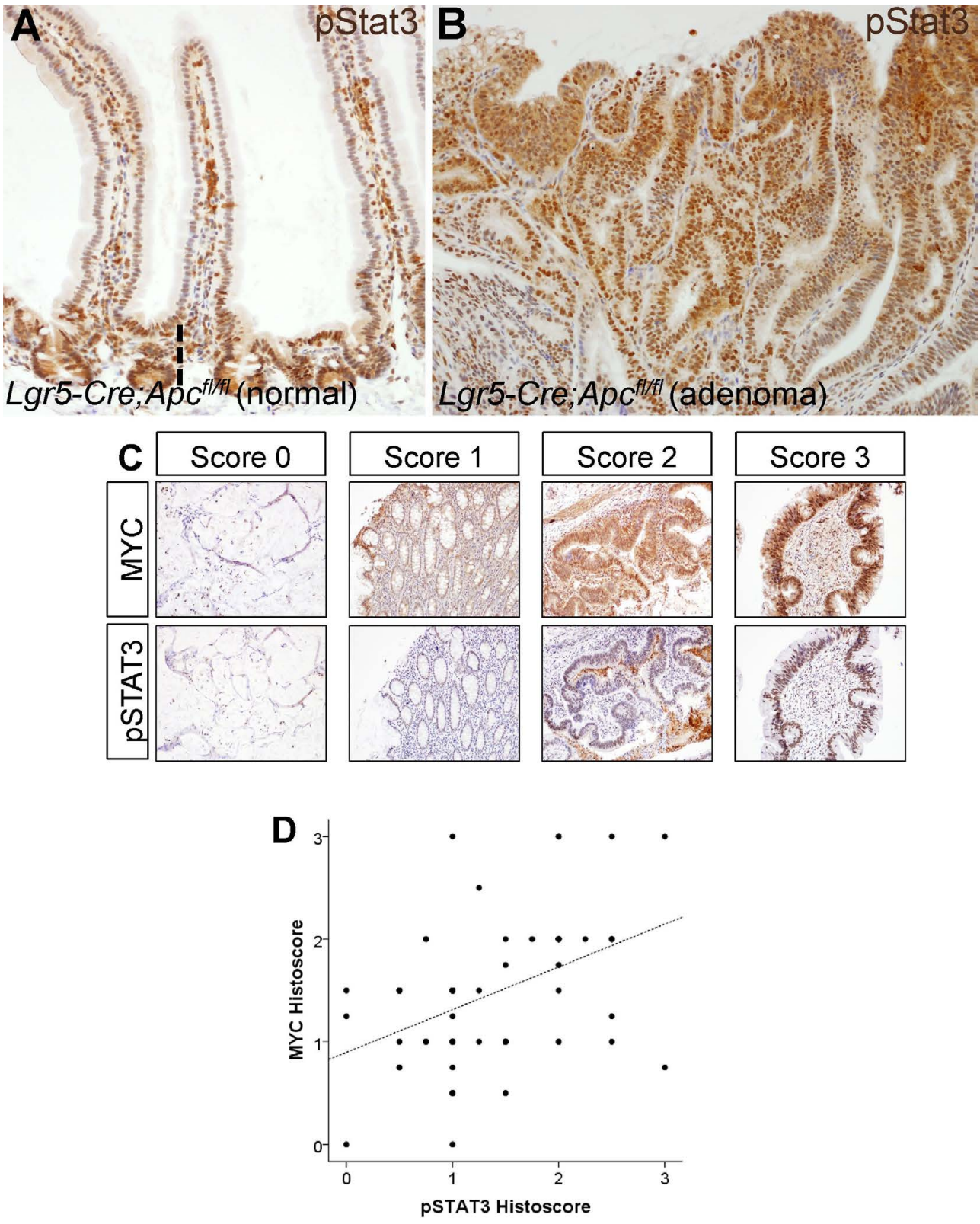

Fig. S6. Stat3 activation in mouse and human colorectal tumor samples. (**A**,**B**) Tissue sections of small intestine from *Lgr5-CreERT2 Apc*$^{fl/fl}$ mice stained with anti-p-Stat3 to look at the activated form of the protein. Examples of normal (A) and transformed (B) areas of the intestine are shown. The dashed line in A indicates the proliferative 'crypt' domain. (**C**,**D**) c-Myc/p-Stat3 correlation analysis in human colorectal TMA. (C) Examples of each of the scores associated with a staining intensity. (D) c-Myc/p-Stat3 staining correlation. Statistical analysis used Spearman's rank correlation coefficient.

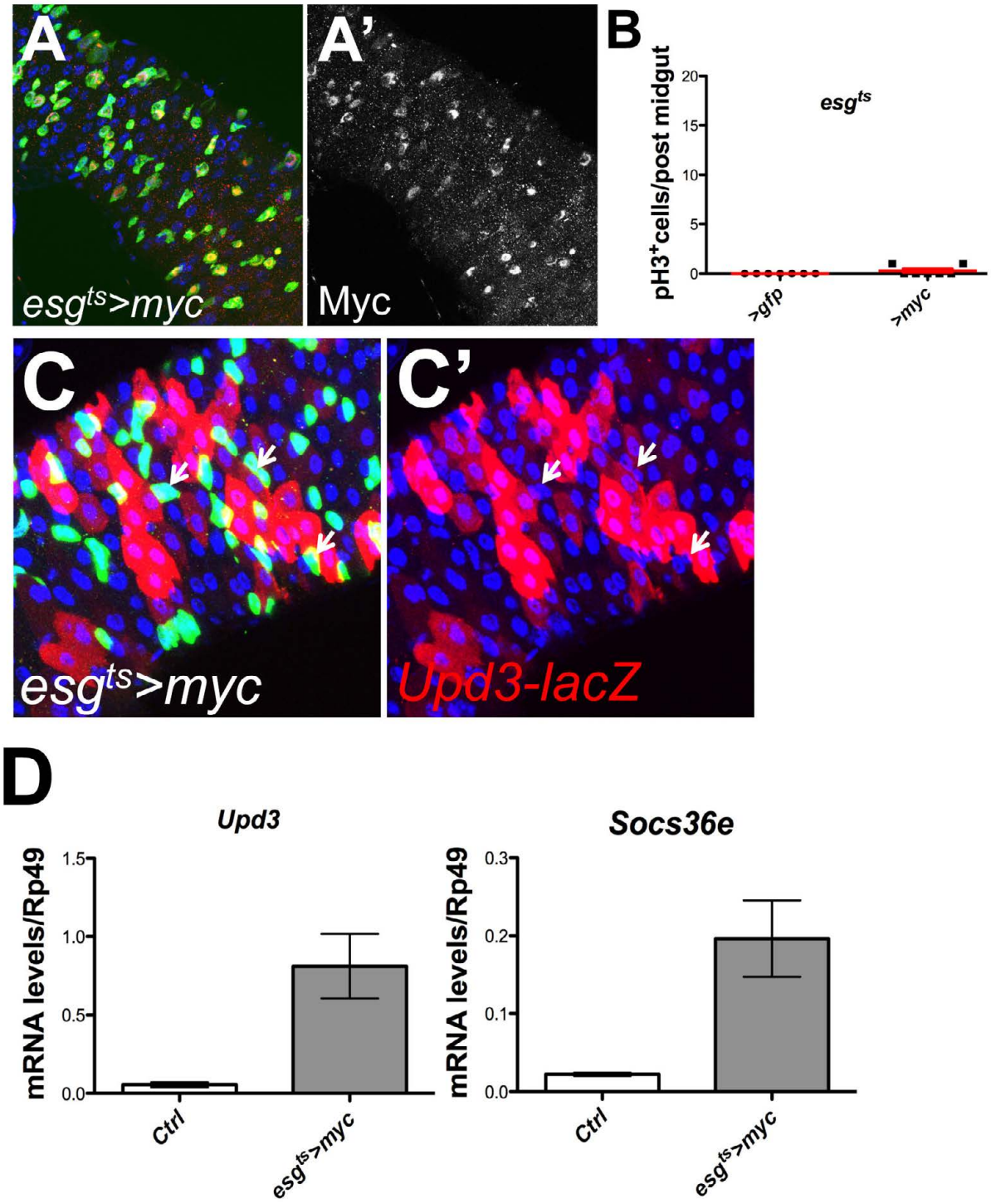

Fig. S7. Myc overexpression recapitulates only some of the phenotypes of high Wnt signaling in the midgut. (**A**,**A**′) Posterior midguts overexpressing Myc in progenitor cells for 14 days (*esg*^{ts}*>myc*) and stained with anti-GFP (green; A) and anti-Myc (red A and white A′). (**B**) Quantification of ISC proliferation from aged-matched *esg*^{ts}*>gfp* and *esg*^{ts}*>myc* intestines represented by the number of pH3^{+} cells/posterior midgut. (**C**,**C**′) Non-cell-autonomous *upd3* expression in ECs in *esg*^{ts}*>myc* midguts monitored with the *upd3-lacZ* reporter (red). Arrows point to *esg*$^{+}$ cells. (**D**) RT-qPCR for *upd3* and *Socs36e* in control and *esg*^{ts}*>myc* midguts after 14 days of transgene expression.

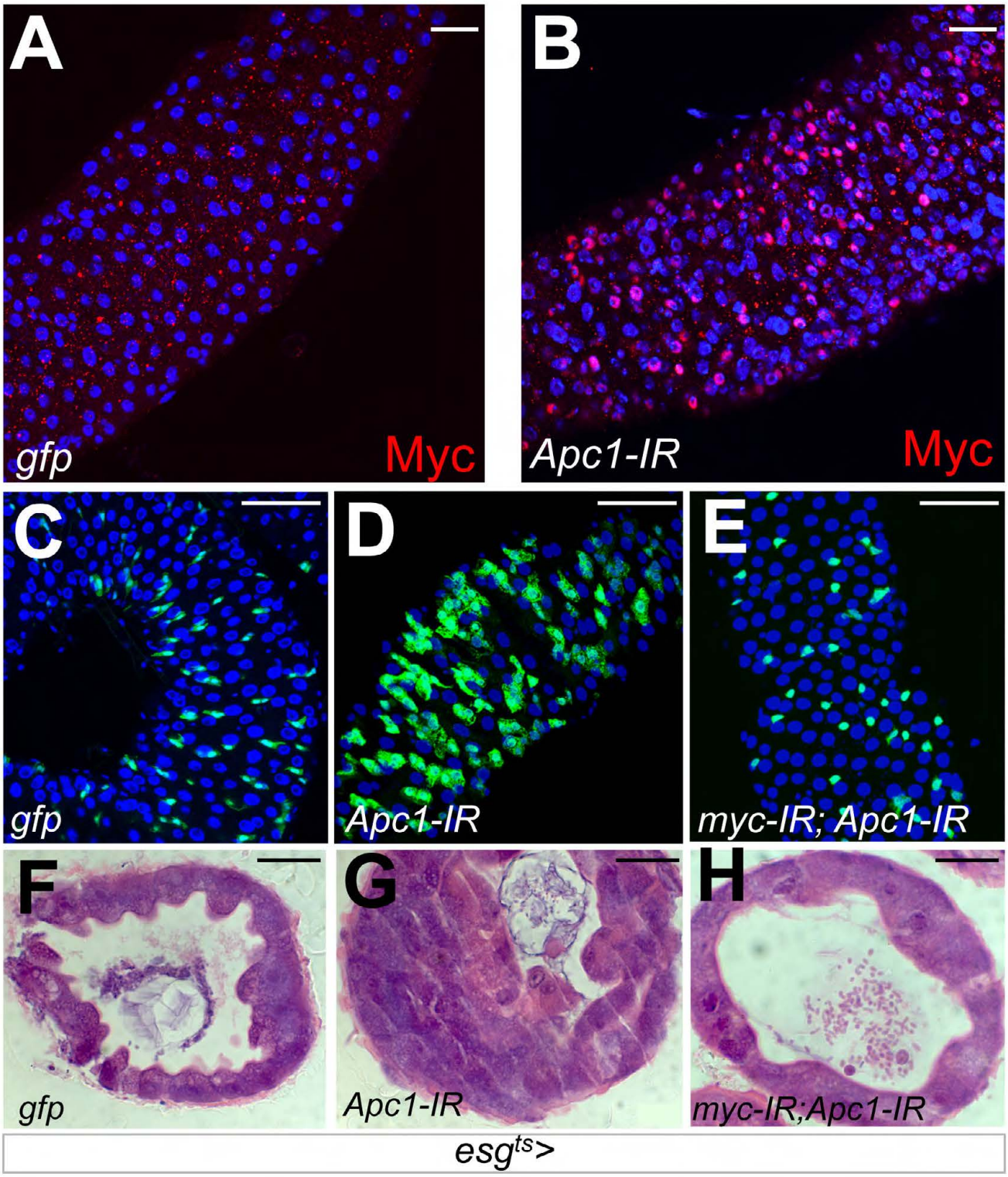

Fig. S8. Myc-dependent ISC proliferation in *esg^{ts}>Apc1-IR* midguts. (**A**,**B**) Posterior midguts of the indicated genotypes after 14 days of transgene overexpression, stained with anti-Myc (red). DAPI (blue) labels nuclei. (**C-E**) Immunofluorescence of midguts of the indicated genotypes after 14 days of transgene overexpression, stained with anti-GFP (green) to label *esg*$^{+}$ cells. (**F-H**) Immunohistochemistry and H+E staining of midguts as in C-E. Scale bars: 20 μm.

Table S1. Primer sequences

Primer	Sequence
RpL32 f	AGGCCCAAGATCGTGAAGAA
RpL32 r	TGTTGCACCAGGAACTTCTTGAA
upd f	CCACGTAAGTTTGCATGTTG
upd r	CTAAACAGTAGCCAGGACTC
upd2 f	ACTGTTGCATGTGGATGCTG
upd2 r	CAGCCAAGGACGAGTTATCA
upd3 f	AGGCCATCAACCTGACCAAC
upd3 r	ACGCTTCTCCATCAGCTTGC
Socs36e f	ATGACCGTGCACTCGCAAAT
Socs36e r	CCTCGTAGCGGTCCATCTTG
spitz f	TACCAGGCATCGAAGGTTTC
spitz r	GACCCAGGCTCCAGTCACTA
vein f	GTGAAGTTGCCTGGATTCGT
vein r	CTACAGGGAGCGACTGATGC
Keren f	CGAGCCATCAATCTCCTTGT
Keren r	AACGATGGCACCTGCTTTAC